Published for SISSA by Springer

Received: May 18, 2020
Revised: July 16, 2020
Accepted: July 24, 2020
Published: August 27, 2020

Search for a light pseudoscalar Higgs boson in the boosted $\mu\mu\tau\tau$ final state in proton-proton collisions at $\sqrt{s} = 13\,\text{TeV}$



The CMS collaboration

E-mail: cms-publication-committee-chair@cern.ch

Abstract: A search for a light pseudoscalar Higgs boson (a) decaying from the 125 GeV (or a heavier) scalar Higgs boson (H) is performed using the 2016 LHC proton-proton collision data at $\sqrt{s} = 13\,\text{TeV}$, corresponding to an integrated luminosity of $35.9\,\text{fb}^{-1}$, collected by the CMS experiment. The analysis considers gluon fusion and vector boson fusion production of the H, followed by the decay $\text{H} \to \text{aa} \to \mu\mu\tau\tau$, and considers pseudoscalar masses in the range $3.6 < m_\text{a} < 21\,\text{GeV}$. Because of the large mass difference between the H and the a bosons and the small masses of the a boson decay products, both the $\mu\mu$ and the $\tau\tau$ pairs have high Lorentz boost and are collimated. The $\tau\tau$ reconstruction efficiency is increased by modifying the standard technique for hadronic τ lepton decay reconstruction to account for a nearby muon. No significant signal is observed. Model-independent limits are set at 95% confidence level, as a function of m_a, on the branching fraction ($\mathcal{B}$) for $\text{H} \to \text{aa} \to \mu\mu\tau\tau$, down to $1.5\,(2.0) \times 10^{-4}$ for $m_\text{H} = 125\,(300)\,\text{GeV}$. Model-dependent limits on $\mathcal{B}(\text{H} \to \text{aa})$ are set within the context of two Higgs doublets plus singlet models, with the most stringent results obtained for Type-III models. These results extend current LHC searches for heavier a bosons that decay to resolved lepton pairs and provide the first such bounds for an H boson with a mass above 125 GeV.

Keywords: Beyond Standard Model, Hadron-Hadron scattering (experiments), Higgs physics

ArXiv ePrint: 2005.08694

Open Access, Copyright CERN,
for the benefit of the CMS Collaboration.
Article funded by SCOAP[3].

https://doi.org/10.1007/JHEP08(2020)139

Contents

1 Introduction 1

2 The CMS detector 3

3 Data and simulated samples 4

4 Event reconstruction 4
- 4.1 Muons 5
- 4.2 Jets 5
- 4.3 Hadronic τ lepton decays 5
- 4.4 Charged lepton efficiency 6

5 Event selection 7

6 Signal and background modeling 7

7 Systematic uncertainties 11

8 Results 15

9 Summary 17

The CMS collaboration 24

JHEP08(2020)139

1 Introduction

Studies of the properties of the 125 GeV Higgs boson can be used to constrain models that include extended Higgs sectors beyond the standard model (SM) [1–5]. Examples include an extension of two Higgs doublets models (2HDM) [6] with a scalar singlet (2HDM+S) [7], the next-to-minimal supersymmetric SM (NMSSM) [8], and pure Higgs sector models containing additional Higgs fields [7]. Especially interesting are models with Higgs boson decay modes that are not detected in the standard channels, which focus on decays to SM particle pairs and invisible decay modes. A recent study by the CMS Collaboration [9] considers models where the Higgs sector contains only doublets and singlets, and the various couplings are otherwise free to vary with respect to their SM values. That analysis reports an upper limit of 0.47 on the branching fraction ($\mathcal{B}$) of the Higgs boson to undetected modes (that is, any mode besides $\gamma\gamma$, ZZ, WW, $\tau\tau$, and bb) at 95% confidence level (CL), when invisible modes are completely excluded. This upper limit on undetected modes strengthens as the upper limit on invisible modes weakens.

Given the weak limits on the branching fraction to undetected final states, it is important to explicitly explore all possibilities for unseen decay modes. Among the most prominent possibilities [10, 11] are decays of the type $\mathrm{H} \to \mathrm{aa}$ or $\mathrm{H} \to \mathrm{hh}$ [12], where H is a scalar Higgs boson and a (h) is a lighter pseudoscalar (scalar) Higgs boson. Such decays are possible in the SM extensions listed above, and generically have large branching fractions when kinematically allowed. However, such decays are not possible in the CP-conserving minimal supersymmetric SM (MSSM) [13]. In what follows, we refer to the light a and h bosons collectively as the a boson. The Higgs boson observed at 125 GeV can be either the lightest or second-lightest scalar [8]. Given observation of the 125 GeV Higgs boson, more recent theoretical studies [7, 14–27] consider the possible decays of this Higgs boson to a pair of lighter Higgs bosons. In all of these models (aside from the MSSM), it is possible for the lightest Higgs (pseudo)scalar boson to be much lighter than the SM-like Higgs boson. If the light Higgs boson is a scalar then the SM-like Higgs boson should be identified with the second-lightest scalar of the model. In the specific case of the NMSSM, a light pseudoscalar boson arises naturally when model parameters are chosen so that there is either a Peccei-Quinn or R global symmetry of the model [8, 10, 11]. Either symmetry will be spontaneously broken by the Higgs vacuum expectation values leading to a massless Nambu-Goldstone boson. After radiative corrections a nearly massless pseudoscalar, the a, emerges. Experimental search results are typically presented for four types of 2HDM (and thus 2HDM+S), differentiated by the couplings of SM fermions to the two doublet fields, Φ_1 and Φ_2, and by their dependence on the ratio of vacuum expectations for the two Higgs doublets, $\tan\beta$. In particular, the NMSSM corresponds to Type-II 2HDM+S, while for Type-III 2HDM+S only the charged leptons couple to Φ_1, which yields enhanced rates, especially at large values of $\tan\beta$. We note that in searches performed so far, the event selection and detection efficiencies for the hh case are essentially the same as for aa. In addition, the branching fractions for h decays are nearly the same as for a decays. Finally, the possibility of additional scalar Higgs bosons with masses above 125 GeV is motivated in generic 2HDM+S [7, 28].

Limits from the CERN LEP experiments on the production of a light scalar boson [29–31] are evaded if the h is singlet-dominated, as required in the limit where the 125 GeV state is SM-like [21, 27, 32]. LEP2 limits on a scalar boson decaying to two light pseudoscalars are obtained for Higgs boson mass (m_{H}) less than 107 GeV [33]. Several searches for different scenarios involving light (pseudo)scalar bosons have been performed by the CERN LHC experiments. The CMS [34] (based on ref. [35]) and LHCb [36] Collaborations place limits on the proton-proton (pp) production of a light pseudoscalar decaying to $\mu\mu$, $\sigma(\mathrm{pp} \to \mathrm{a})\mathcal{B}(\mathrm{a} \to \mu\mu)$, that significantly constrain the MSSM-like fraction of the NMSSM pseudoscalar state, especially at large $\tan\beta$. Nonetheless, large $\mathcal{B}(\mathrm{H} \to \mathrm{aa})$ remains possible. Direct constraints on $\mathcal{B}(\mathrm{H} \to \mathrm{aa})$ are obtained by CMS [37] and ATLAS [38] based on the 4μ final state and by CMS [39] using the $\mu\mu\tau\tau$, 4τ, and $\mu\mu\mathrm{bb}$ final states. Analyses especially relevant for pseudoscalar masses, m_{a}, greater than twice the τ lepton mass, m_τ, are based on the $\mu\mu\tau\tau$, $\mathrm{bb}\tau\tau$, 4τ, and 4b final states and have been performed by the CMS [40–42] and ATLAS [43–45] Collaborations.

The analysis presented in this paper considers $\mu\mu\tau\tau$ final states arising from $\mathrm{H} \to \mathrm{aa} \to \mu\mu\tau\tau$, where SM-like production of the H boson via the dominant gluon fusion

JHEP08(2020)139

(ggF) and vector boson fusion (VBF) modes are both included [46]. This analysis focuses on the pseudoscalar boson mass range 3.6–21 GeV, complementary to searches, such as ref. [40], that focus on heavier pseudoscalar masses. For light masses, the large Lorentz boost of the a boson causes its decay products to overlap. In the $\mu\mu$ channel, the standard CMS muon identification has sensitivity to the topology of boosted muon pairs similar to that for an isolated, nonboosted muon pair. To reconstruct the collimated τ lepton pair, we have developed a boosted τ lepton pair reconstruction technique to target the specific decay where one τ lepton decays to a muon and neutrinos, τ_μ, while the other decays to one or more hadrons and a neutrino, τ_h, thus: a $\to \tau_\mu\tau_\mathrm{h}$. This technique improves upon the standard CMS τ lepton reconstruction that is optimized for isolated, nonboosted τ leptons. The $\mu\mu\tau_\mu\tau_\mathrm{h}$ channel has greater detection efficiency than final states with b quarks, which are difficult to reconstruct at low momentum and significant boost, and has a larger branching fraction than most models with four-muon final states. The effectiveness of this improved technique also makes possible for the first time the search for the decays of a heavier Higgs boson to aa in the $\mu\mu\tau\tau$ final state at low m_a, with $m_\mathrm{H} = 300$ GeV used as a demonstration. Such an H boson generically has a large branching fraction to any kinematically accessible pair of lighter bosons [28, 47]; the light bosons are highly boosted and the resulting final-state leptons are similarly collimated. The search is performed using an unbinned parameterized maximum likelihood fit of signal and background contributions to the two-dimensional (2D) distribution of the $\mu\mu$ invariant mass $m(\mu\mu)$ and the 4-body visible mass $m(\mu\mu\tau_\mu\tau_\mathrm{h})$.

This paper is organized as follows. A brief description of the CMS detector is given in section 2. Section 3 summarizes the data and simulated samples used. Section 4 describes the object identification algorithms, including the modified $\tau_\mu\tau_\mathrm{h}$ reconstruction technique, while section 5 focusses on the event selection. The background and signal models of the 2D unbinned fit are described in section 6 and the treatment of systematic uncertainties are subsequently discussed in section 7. The model-independent results, as well as interpretation in the context of several 2HDM+S types, are presented in section 8. The paper is summarized in section 9.

2 The CMS detector

The central feature of the CMS apparatus is a superconducting solenoid of 6 m internal diameter, providing a magnetic field of 3.8 T. Within the solenoid volume are a silicon pixel and strip tracker, a lead tungstate crystal electromagnetic calorimeter (ECAL), and a brass and scintillator hadron calorimeter, each composed of a barrel and two endcap sections. Forward calorimeters extend the pseudorapidity (η) coverage provided by the barrel and endcap detectors. Muons are measured in gas-ionization detectors embedded in the steel flux-return yoke outside the solenoid. Events of interest are selected using a two-tiered trigger system [48]. The first level (L1), composed of custom hardware processors, uses information from the calorimeters and muon detectors to select events at a rate of around 100 kHz within a time interval of less than 4 μs. The second level, known as the high-level trigger (HLT), consists of a farm of processors running a version of the full event

JHEP08(2020)139

reconstruction software optimized for fast processing, and reduces the event rate to around 1 kHz before data storage. A more detailed description of the CMS detector, together with a definition of the coordinate system used and the relevant kinematic variables, can be found in ref. [49].

3 Data and simulated samples

This search uses a sample of pp collisions at the LHC, collected in 2016 at $\sqrt{s} = 13\,\text{TeV}$, corresponding to an integrated luminosity of $35.9\,\text{fb}^{-1}$.

The acceptance and reconstruction efficiency of the $\text{H} \to \text{aa} \to \mu\mu\tau\tau$ processes are evaluated using simulated events. These signal processes are generated with MadGraph5_aMC@NLO version 2.2.2 [50] at next-to-leading order (NLO). The pythia 8.205 program [51] is used for parton showering, hadronization, and the underlying event is simulated with the CUETP8M1 tune [52]. The NNPDF3.0 [53] set of parton distribution functions is used. Samples are generated for $3.6 < m_\text{a} < 21\,\text{GeV}$ for the SM-like H boson with $m_\text{H} = 125\,\text{GeV}$, and for $5 < m_\text{a} < 21\,\text{GeV}$ for a heavier H boson with $m_\text{H} = 300\,\text{GeV}$. The ggF Higgs production process is simulated for each sample with the obtained signal yields scaled to the sum of the expected events from ggF and VBF processes. The VBF Higgs production process is simulated for a subset of the H and a boson mass pairs. The inclusion of the VBF process increases the expected signal yield by 8 (19)% for $m_\text{H} = 125\,(300)\,\text{GeV}$. An acceptance correction arising from a small difference in the analysis acceptance for ggF and VBF events of 0.5–3.0% is applied as a function of Higgs and pseudoscalar boson masses, with an uncertainty of 0.5%. This correction primarily arises from the differences in transverse momentum p_T spectrum of the generated H and a bosons. These differences have a negligible effect on the shapes of the reconstructed pseudoscalar mass distributions that are used to discriminate signal from background. The WH, ZH, and $\text{t}\bar{\text{t}}\text{H}$ Higgs boson production modes do not significantly increase the sensitivity of this search due to lower cross sections and reduced acceptance and are not included.

For all processes, the detector response is simulated using a detailed description of the CMS detector, based on the Geant4 package [54], and the event reconstruction is performed with the same algorithms used for data. The simulated samples include additional interactions per bunch crossing (pileup) and are weighted so that the multiplicity distribution matches the measured one, with an average of about 23 interactions per bunch crossing.

4 Event reconstruction

Using the information from all CMS subdetectors, a particle-flow (PF) technique is employed to identify and reconstruct the individual particles emerging from each collision [55]. The particles are classified into mutually exclusive categories: charged and neutral hadrons, photons, muons, and electrons. Jets and τ_h candidates are identified algorithmically using the PF-reconstructed particles as inputs. The missing transverse momentum vector $\vec{p}_\text{T}^{\,\text{miss}}$ is defined as the projection onto the plane perpendicular to the beam axis of the negative vector sum of the momenta of all reconstructed PF objects in an event. Its magnitude

JHEP08(2020)139

is referred to as $p_{\mathrm{T}}^{\mathrm{miss}}$. The primary pp interaction vertex is defined as the reconstructed vertex with the largest value of summed physics-object p_{T}^2. The physics objects considered in the vertex determination are the objects returned by a jet finding algorithm [56, 57] applied to all charged tracks associated with the vertex, plus the corresponding associated $p_{\mathrm{T}}^{\mathrm{miss}}$, taken as the negative vector sum of the p_{T} of those jets. Finally, additional identification criteria are applied to the reconstructed muons, electrons, photons, τ_{h} candidates, jets, and $p_{\mathrm{T}}^{\mathrm{miss}}$ to reduce the frequency of misidentified objects. This section details the reconstruction and identification of muons, jets, and τ_{h} candidates.

4.1 Muons

Muons are reconstructed within $|\eta(\mu)| < 2.4$ [58]. The reconstruction combines the information from both the tracker and the muon spectrometer. The muons are selected from among the reconstructed muon track candidates by applying minimal requirements on the track components in the muon system and taking into account matching with small energy deposits in the calorimeters. For each muon track, the distance of closest approach to the primary vertex in the transverse plane is required to be less than 0.2 cm. The distance of closest approach to the primary vertex along the beamline, d_{z}, must be less than 0.5 cm.

The isolation of individual muons is defined relative to their transverse momentum $p_{\mathrm{T}}(\mu)$ by summing over the p_{T} of charged hadrons and neutral particles within a cone around the muon direction at the interaction vertex with radius $\Delta R = \sqrt{(\Delta\eta)^2 + (\Delta\phi)^2} < 0.4$ (where ϕ is the azimuthal angle in radians) :

$$I^{\mu} = \left(\sum p_{\mathrm{T}}^{\mathrm{charged}} + \max\left[0, \sum p_{\mathrm{T}}^{\mathrm{neutral}} + \sum p_{\mathrm{T}}^{\gamma} - p_{\mathrm{T}}^{\mathrm{PU}}\right] \right) / p_{\mathrm{T}}(\mu). \tag{4.1}$$

Here, $\sum p_{\mathrm{T}}^{\mathrm{charged}}$ is the scalar p_{T} sum of charged hadrons originating from the primary vertex. The $\sum p_{\mathrm{T}}^{\mathrm{neutral}}$ and $\sum p_{\mathrm{T}}^{\gamma}$ are the scalar p_{T} sums for neutral hadrons and photons, respectively. The neutral contribution to the isolation from pileup interactions, $p_{\mathrm{T}}^{\mathrm{PU}}$, is estimated as $0.5 \sum_i p_{\mathrm{T}}^{\mathrm{PU},i}$, where i runs over the charged hadrons originating from pileup vertices and the factor 0.5 corrects for the ratio of charged to neutral particle contributions in the isolation cone. Muons are considered isolated if $I^{\mu} < 0.25$.

4.2 Jets

Jets are reconstructed using PF objects. The anti-k_{T} jet clustering algorithm [56, 57] with a distance parameter of 0.4 is used. The standard method for jet energy corrections [59] is applied. In order to reject jets coming from pileup collisions, a multivariate (MVA) jet identification algorithm [60] is applied. This algorithm takes advantage of differences in the shapes of energy deposits in a jet cone between pileup jets and jets originating from a quark or gluon. The combined secondary vertices (CSV) b tagging algorithm [61] is used to identify jets originating from b hadrons [62]. The efficiency for tagging b jets is ≈63%, while the misidentification probability for charm (light-quark or gluon) jets is ≈12 (1)%.

4.3 Hadronic τ lepton decays

Hadronically decaying τ leptons are reconstructed and identified within $|\eta(\tau_{\mathrm{h}})| < 2.3$ using the hadron-plus-strips (HPS) algorithm [63], which targets the main decay modes by

JHEP08(2020)139

selecting PF objects with one charged hadron and up to two neutral pions, or with three charged hadrons. The HPS algorithm is seeded by the jets described in section 4.2. The τ_h candidates are reconstructed based on the number of tracks and on the number of ECAL strips with an energy deposit in the η-ϕ plane.

This analysis uses a specialized $\tau_\mu\tau_h$ reconstruction algorithm, which uses the same HPS method as the above, with a modified jet seed. This method is designed to reconstruct boosted $\tau_\mu\tau_h$ objects, for which the τ lepton decaying leptonically to a muon overlaps with the hadronic decay products of the other τ lepton. One τ lepton is required to decay to a muon because this mode has a high reconstruction efficiency and a low misidentification probability. As in ref. [39], a joint reconstruction of the τ_h candidate and a nearby muon is performed. Jets that seed the τ_h reconstruction are first modified to remove muons with $p_T > 3\,\text{GeV}$ passing minimal identification requirements from their jet constituents. The τ_h candidates reconstructed using these modified jets are required to have $p_T > 10\,\text{GeV}$, where the reconstructed $p_T(\tau_h)$ corresponds to the visible portion of the τ lepton decay. To reject τ_h candidates that arise from constituents not originating from the primary vertex, the τ_h candidates must have $d_z < 0.5\,\text{cm}$. To reduce background contribution from jets arising from b quarks, the jet seeds to the τ_h reconstruction must additionally fail the CSV jet tagging algorithm. Because no MVA discriminant to reject electrons [63] is applied, the τ_h reconstruction algorithm has high efficiency to select τ leptons that decay to electrons, τ_e. The fraction of reconstructed τ_h candidates that are τ_e decays is estimated from simulation to be 18–22%, predominantly reconstructed in the one-prong decay mode with no additional neutral hadrons. No distinction is made between τ_e and τ_h candidates and this paper refers to the contribution of both decay categories as τ_h candidates.

The full $\tau_\mu\tau_h$ identification procedure includes the modified HPS algorithm described above, along with a requirement on the τ_h candidate isolation. The isolation of a τ_h candidate is computed using an MVA discriminant [63]. The discriminant is computed using PF candidates, with the overlapping muon excluded, in the region around the τ_h candidate defined by $\Delta R < 0.8$. The τ_h candidates are required to pass a selection on the MVA discriminant output as a function of $p_T(\tau_h)$ to yield an approximately constant efficiency of ≈80%. No discriminant to reject muons [63] is applied, as it would reduce the reconstruction efficiency of the boosted $\tau_\mu\tau_h$ final state.

4.4 Charged lepton efficiency

The combined efficiencies of the reconstruction, identification, and isolation requirements for muons are measured in several bins of $p_T(\mu)$ and $|\eta(\mu)|$ using a "tag-and-probe" technique [64] applied to an inclusive sample of muon pairs from Z boson and J/ψ meson events [58]. These efficiencies are measured in data and simulation. The data to simulation efficiency ratios are used as scale factors to correct the simulated event yields. For τ_h candidates, two scale factors are similarly measured using a $Z \to \tau_\mu\tau_h$ sample [63] to be $0.60 \pm 0.11\,(0.97 \pm 0.05)$ for $10 < p_T(\tau_h) < 20\,\text{GeV}$ ($p_T(\tau_h) > 20\,\text{GeV}$), which are found to be independent of $|\eta(\tau_h)|$. For $10 < p_T(\tau_h) < 20\,\text{GeV}$, the $Z \to \tau_\mu\tau_h$ data sample contains significant W+jets background, making the scale factor difficult to estimate with as high a precision as for $p_T(\tau_h) > 20\,\text{GeV}$.

JHEP08(2020)139

5 Event selection

Collision events are selected by a trigger that requires the presence of an isolated muon with $p_{\mathrm{T}} > 24\,\mathrm{GeV}$ [48]. Trigger efficiencies are measured in data and simulation using the tag-and-probe technique. The event is required to have two isolated opposite-sign muons with $\Delta R < 1$. The leading muon which is matched to the muon that triggered the event must have $p_{\mathrm{T}} > 26\,\mathrm{GeV}$. The second muon must have $p_{\mathrm{T}} > 3\,\mathrm{GeV}$. These muons constitute a $\mu\mu$ pair from one of the pseudoscalar candidates.

The second pseudoscalar is selected via its decay to an isolated opposite-sign $\tau_\mu\tau_{\mathrm{h}}$ pair. The $\tau_\mu\tau_{\mathrm{h}}$ selection requires one identified muon with $p_{\mathrm{T}} > 3\,\mathrm{GeV}$, with no isolation selection imposed, and one τ_{h} candidate with $p_{\mathrm{T}} > 10\,\mathrm{GeV}$, reconstructed as described in section 4.3. The reconstructed muon corresponds to the visible portion of the τ_μ decay. The two τ lepton candidates are required to lie within $\Delta R(\tau_\mu, \tau_{\mathrm{h}}) < 0.8$. The value of 0.8 is driven by the modified HPS algorithm isolation discriminant and ensures the boosted topology. This selection, with the corresponding selection of the $\mu\mu$ pair, prevents combinatoric background in which the wrong combination of leptons is assigned to the pseudoscalar candidates. The $\mu\mu$ pair selection is looser to avoid loss of efficiency.

The modified $\tau_\mu\tau_{\mathrm{h}}$ reconstruction and identification algorithm increases the signal efficiency throughout the full range of Higgs boson and pseudoscalar hypotheses considered, as shown in figure 1. The efficiency of the $\tau_\mu\tau_{\mathrm{h}}$ reconstruction and identification is measured by requiring the presence of a muon passing the identification requirements and a τ_{h} candidate passing either the standard τ_{h} HPS reconstruction or the $\tau_\mu\tau_{\mathrm{h}}$ HPS reconstruction, as well as the MVA isolation discriminant. The increase in efficiency arises incrementally both from the modification of the jets which seed the $\tau_\mu\tau_{\mathrm{h}}$ reconstruction and the exclusion of the muon energy from the MVA isolation discriminant. Because of the increase in Lorentz boost, the jet seed modification is the primary cause of increased efficiency at low m_{a} where the pseudoscalar decay products are most overlapping, with $\Delta R(\tau_\mu, \tau_{\mathrm{h}}) < 0.4$. At larger separation, $0.4 < \Delta R(\tau_\mu, \tau_{\mathrm{h}}) < 0.8$, the change in the MVA discriminant becomes the only source of efficiency increase. The reduced efficiency at low pseudoscalar mass is due to the high Lorentz boost in which the muon is nearly collinear with a charged hadron from the τ_{h} candidate. At low Lorentz boost, the muon and τ_{h} candidate have a large separation. In this case, the efficiency is reduced from the requirement of the boosted topology, especially at $m_{\mathrm{H}} = 125\,\mathrm{GeV}$. The efficiency for the higher H boson mass is less affected by an increase in pseudoscalar mass because the reduction in Lorentz boost is generally not significant enough to separate the τ leptons from a pseudoscalar decay beyond the selection requirement of $\Delta R(\tau_\mu, \tau_{\mathrm{h}}) < 0.8$.

6 Signal and background modeling

The main source of background in this search is Drell-Yan $\mu\mu$ production in association with at least one jet that is misidentified as the $\tau_\mu\tau_{\mathrm{h}}$ candidate. This background, reduced by the $\tau_\mu\tau_{\mathrm{h}}$ reconstruction, features the prominent $\mu\mu$ resonances with masses between 3.6 and 21 GeV: $\psi(2S)$ (3.69 GeV), $\Upsilon(1S)$ (9.46 GeV), $\Upsilon(2S)$ (10.0 GeV),

JHEP08(2020)139

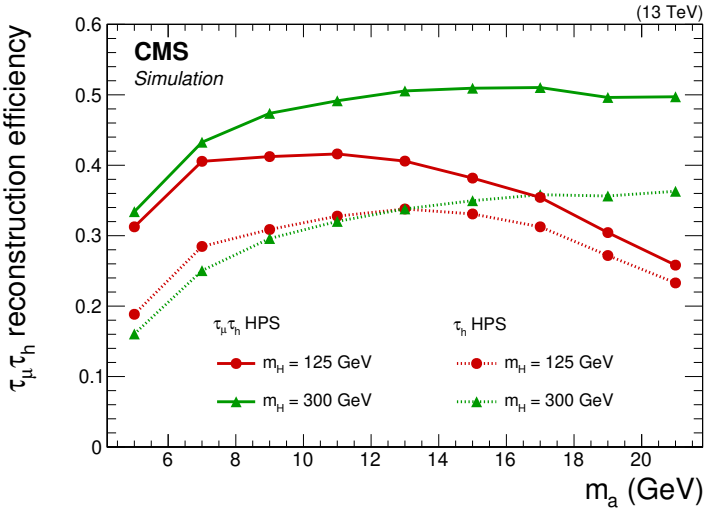


Figure 1. The efficiency of the standard HPS (dashed lines) and $\tau_\mu\tau_h$ HPS reconstruction used in this search (solid lines) as a function of pseudoscalar boson mass for $m_H = 125$ (red) and 300 GeV (green). The events are required to have two reconstructed muons passing identification and isolation criteria. The efficiency is measured by additionally requiring a third muon passing identification requirements and a τ_h candidate reconstructed using either the standard HPS algorithm or the $\tau_\mu\tau_h$ HPS algorithm and passing isolation requirements.

and $\Upsilon(3S)$ (10.4 GeV) [65]. In the $m(\mu\mu)$ distribution, the known resonance peaks appear on top of the Drell-Yan continuum. In the $m(\mu\mu\tau_\mu\tau_h)$ distribution, the $\mu\mu$ + jet background appears as an exponentially falling distribution with a threshold around 40–60 GeV because of the p_T thresholds of the three reconstructed muons and one τ_h candidate. The signal is characterized by a narrow $m(\mu\mu)$ resonance from a pseudoscalar decay and a broader $m(\mu\mu\tau_\mu\tau_h)$ distribution because of the invisible decay products of one of the pseudoscalar Higgs bosons. As described below, the search strategy consists of an unbinned fit of $m(\mu\mu)$ vs. $m(\mu\mu\tau_\mu\tau_h)$, using analytical models for the signal and background shapes in each dimension. The background shape model for the Drell-Yan continuum, the meson resonances mentioned above, and additionally the J/ψ resonance (3.10 GeV [65]) are constrained via a data control region enriched in $\mu\mu$+jet events. Although the J/ψ resonance falls outside the kinematically allowed search window for a $\tau\tau$ resonance, it is modeled in the fit to provide a better background description near the $\psi(2S)$ meson.

The analysis uses a simultaneous unbinned fit of three mutually exclusive regions to model the background and search for a signal. The "control region" requires the presence of two muons and no identified $\tau_\mu\tau_h$ candidate. The next two regions additionally require a reconstructed $\tau_\mu\tau_h$ candidate and are defined by passing or failing the τ_h MVA isolation requirement, labeled as "signal region" and "sideband", respectively. A schematic depiction of the three regions is shown in figure 2. Two additional regions are also shown and are used to validate the background estimation method described below.

The choice of $m(\mu\mu)$ and $m(\mu\mu\tau_\mu\tau_h)$ as observables for distinguishing the $H \to aa$ signal from the SM background processes is found to be more performant than combinations

JHEP08(2020)139

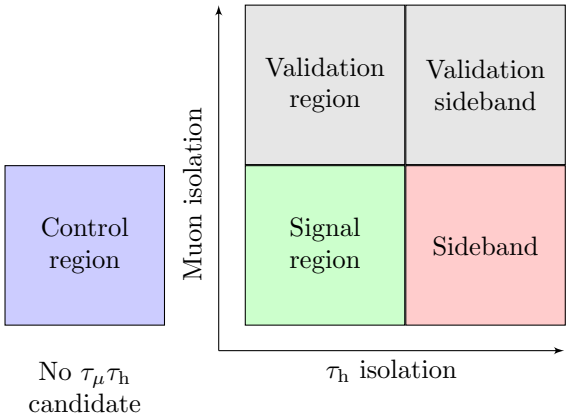


Figure 2. Schematic of the fit regions in the analysis. Events with two isolated muons and no $\tau_\mu\tau_h$ candidates constitute the control region (blue). Events that have a $\tau_\mu\tau_h$ candidate are further divided based on the isolation of the τ_h candidate with isolated $\tau_\mu\tau_h$ candidates forming the signal region (green) and the remaining $\tau_\mu\tau_h$ candidates forming the sideband (red). Additionally, the $\mu\mu$ candidates that fail the muon isolation selection form two analogous regions for the validation of the background fit model (gray).

including $m(\tau_\mu\tau_h)$ over the largest range of Higgs boson and pseudoscalar mass hypotheses. The signal is modeled as a 2D function given by the product of a Voigt function for $m(\mu\mu)$ and a split normal distribution for $m(\mu\mu\tau_\mu\tau_h)$. For the signal processes, there is minimal correlation between the $m(\mu\mu)$ and $m(\mu\mu\tau_\mu\tau_h)$ distributions. The parameters of the model are determined from fits to the signal simulation. Each generated distribution, with a specified Higgs boson and pseudoscalar mass, is fit with the described 2D function. For each parameter, a polynomial function is used to interpolate between the generated masses: a first-order polynomial for the mean value of the $m(\mu\mu)$ and $m(\mu\mu\tau_\mu\tau_h)$, a second-order polynomial for each width parameter, and the product of a first-order polynomial and two error functions for the signal normalization. The search is performed for pseudoscalar masses between 3.6 and 21 GeV.

The 2D fit of $m(\mu\mu)$ vs. $m(\mu\mu\tau_\mu\tau_h)$ is performed in data to model the SM background processes and extract any significant signal process contribution in three ranges of the $m(\mu\mu)$ spectrum: $2.5 < m(\mu\mu) < 8.5\,\text{GeV}$, $6 < m(\mu\mu) < 14\,\text{GeV}$, and $11 < m(\mu\mu) < 25\,\text{GeV}$. For a given m_a, a single $m(\mu\mu)$ range is used, with the transition between the $m(\mu\mu)$ ranges occurring at $m_a = 8$ and 11.5 GeV. There is some overlap in the fit ranges to allow the lower or upper portion of the signal model to be fully contained in the given fit range. The background probability density function (PDF) used for the $m(\mu\mu)$ spectrum is the sum of an exponential together with two, three, or zero Voigt distributions to model the SM resonances for the three respective ranges. An additional exponential function is necessary to model the rising continuum background near the J/ψ resonance in the lowest $m(\mu\mu)$ range. The $m(\mu\mu\tau_\mu\tau_h)$ background distribution is modeled with the product of an error function and the sum of two exponential distributions. The second exponential provides the fit with additional flexibility to allow the fit to favor an extended tail if necessary. The fit range is $0 < m(\mu\mu\tau_\mu\tau_h) < 1200\,\text{GeV}$ in all three $m(\mu\mu)$

JHEP08(2020)139

ranges. The $m(\mu\mu)$ and $m(\mu\mu\tau_\mu\tau_h)$ functions are multiplied together to produce a 2D PDF. Because $m(\mu\mu\tau_\mu\tau_h)$ is loosely correlated with $m(\mu\mu)$ in the background distribution, the parameters of the $m(\mu\mu\tau_\mu\tau_h)$ background model in a given $m(\mu\mu)$ range are allowed to vary independently of the other ranges, allowing a correlation between $m(\mu\mu)$ and $m(\mu\mu\tau_\mu\tau_h)$.

The normalization of the background model in the signal region is estimated from the sideband using a "tight-to-loose" method. This method uses a $Z(\mu\mu)$ + jet sample to estimate the efficiency for a jet that has passed all the τ_h reconstruction requirements (including the muon removal step) of section 4.3, except the MVA isolation requirement, to additionally pass the MVA isolation requirement. The region contains events collected with a single muon trigger with the requirement of two isolated opposite-sign muons and a jet that has been misidentified as a $\tau_\mu\tau_h$ object with a muon within $\Delta R(\tau_\mu, \tau_h) < 0.8$, without the requirement on the MVA isolation. The $\mu\mu$ pair must have invariant mass $81 < m(\mu\mu) < 101\,\text{GeV}$. The tight-to-loose ratio, f, is defined as the ratio of the number of τ_h candidates that pass the MVA isolation requirement in addition to the other identification requirements (the "tight" condition) to the number of τ_h candidates that pass the other identification requirements, but with a relaxed requirement on the isolation (the "loose" condition). The calculation of f is performed separately for each hadronic decay mode of the τ lepton and is binned in $p_T(\tau_h)$. This region is dominated by Drell-Yan events containing jets. Residual contributions from diboson processes, as estimated from simulation, are subtracted from the data. The associated jets are the objects most likely to pass the τ_h reconstruction criteria. This tight-to-loose ratio is measured to be 10–40%, increasing at lower $p_T(\tau_h)$. In general, the decay mode with three charged tracks has a lower tight-to-loose ratio than those with a single charged track.

The sideband is then reweighted using the tight-to-loose method to estimate the contribution in the signal region. The weights are applied on an event-by-event basis as a function of $p_T(\tau_h)$. The tight-to-loose method is verified in a validation region independent of the analysis region by inverting the isolation requirement on the muon in the $\mu\mu$ pair that did not trigger the event. These regions correspond to the gray boxes in figure 2. The expected and observed yields in this validation region are compatible within 15%, and an uncertainty is derived from this value.

The parameters of the $\mu\mu$ resonances — mean (μ), width (Γ), and resolution (σ)—and the relative normalizations—N_i/N_j where i and j are a pair of background resonances — between the J/ψ and $\psi(2S)$ resonances and between the $\Upsilon(1S)$ and each of the $\Upsilon(2S)$ and $\Upsilon(3S)$ resonances are constrained via a simultaneous fit among all three regions. The parameters of the resonances are compatible, and thus the same, among the three regions, while their relative normalizations are only the same in the sideband and control region with the signal region relative normalizations related to the sideband via a linear transformation. The slope and constant values of this linear transformation are determined from a fit to the sideband and the tight-to-loose estimation of the background in the signal region. An uncertainty is assigned for this linear constraint in the signal region. This uncertainty is derived in a validation region and a corresponding validation sideband in which the muon of the $\mu\mu$ pair which did not trigger the event has an inverted isolation requirement and is

JHEP08(2020)139

Category	Parameters	Signal region	Sideband	Control region
$\mu\mu$ resonances	μ, σ, Γ	Constrained (three regions)		
$\mu\mu$ continuum	$\lambda^{\mathrm{i}}_{\mu\mu}$	Tight-to-loose	Free	Free
$\mu\mu\tau_\mu\tau_\mathrm{h}$	Erf_a, Erf_b, $\lambda^{\mathrm{i}}_{\mu\mu\tau\tau}$	Tight-to-loose	Free	—
Normalizations	$N_{\psi(2\mathrm{S})}/N_{\mathrm{J}/\psi}$	Tight-to-loose	Constrained (two regions)	
	$N_{\Upsilon(2\mathrm{S})}/N_{\Upsilon(1\mathrm{S})}$	Tight-to-loose	Constrained (two regions)	
	$N_{\Upsilon(3\mathrm{S})}/N_{\Upsilon(1\mathrm{S})}$	Tight-to-loose	Constrained (two regions)	
	$N_{\Upsilon(1\mathrm{S})}/N_{\mathrm{J}/\psi}$	Tight-to-loose	Free	Free
	$N_{\mathrm{J}/\psi}/N_{\mathrm{continuum}}$	Tight-to-loose	Free	Free

Table 1. Background model parameters and their relations among the three fit regions in the analysis. The $\mu\mu$ background model includes the five meson resonances modeled using a Voigt function over an exponential continuum. The 4-body background model includes an error function multiplied with the sum of two exponential distributions. Three types of fit region relations are used: (a) constrained, in which the parameters are the same in the indicated regions, (b) free, in which the parameter is not related to those in any other region, and (c) related via the $\tau_\mu\tau_\mathrm{h}$ tight-to-loose ratio, in which the indicated parameter in the signal region is constrained to the corresponding parameter in the sideband via a linear transformation.

measured to be 5–20% depending on the resonance. The parameters of the $\mu\mu$ continuum ($\lambda^{i}_{\mu\mu}$), the $m(\mu\mu\tau_\mu\tau_\mathrm{h})$ continuum ($\lambda^{i}_{\mu\mu\tau\tau}$), the $m(\mu\mu\tau_\mu\tau_\mathrm{h})$ error function shift (Erf_a) and scale (Erf_b), and the relative normalizations of the $\mu\mu$ resonances to the $\mu\mu$ continuum ($N_{\Upsilon(1\mathrm{S})}/N_{\mathrm{J}/\psi}$ and $N_{\mathrm{J}/\psi}/N_{\mathrm{continuum}}$) are constrained in the signal region to the sideband via the tight-to-loose method. All remaining parameters are free to vary independently of each other and share no constraint between regions. Table 1 summarizes these constraints.

The background model and observed data in the control region are shown in figure 3. Projections on the $m(\mu\mu)$ and $m(\mu\mu\tau_\mu\tau_\mathrm{h})$ axes of the 2D background model and observed data with sample signal distributions for each fit range are shown in figures 4 and 5 for the sideband and signal region, respectively. The signal distribution is scaled assuming an SM Higgs boson production cross section [46] and $\mathcal{B}(\mathrm{H} \to \mathrm{aa} \to \mu\mu\tau\tau) = 5 \times 10^{-4}$. A small level of signal contamination is expected in the sideband and is included in the fit. For the signal processes, there is minimal correlation between the $m(\mu\mu)$ and the $m(\mu\mu\tau_\mu\tau_\mathrm{h})$ distributions.

7 Systematic uncertainties

Uncertainties in the signal process modeling contribute both to the total expected signal yield and the individual signal fit parameters. Despite the small spatial separation between the τ_μ and τ_h candidates, the $\tau_\mu\tau_\mathrm{h}$ reconstruction procedure, which relies on the excellent muon discrimination of the CMS detector, allows the uncertainties in the τ_h efficiency and energy scale modeling to be treated independently from those for the τ_μ candidates. Systematic uncertainties in the efficiency measurements from the tag-and-probe technique contribute an uncertainty in the total signal yield of 0.5% for the muon trigger efficiency and 1.0–1.4% for each reconstructed muon. The uncertainty in the muon momentum scale

JHEP08(2020)139

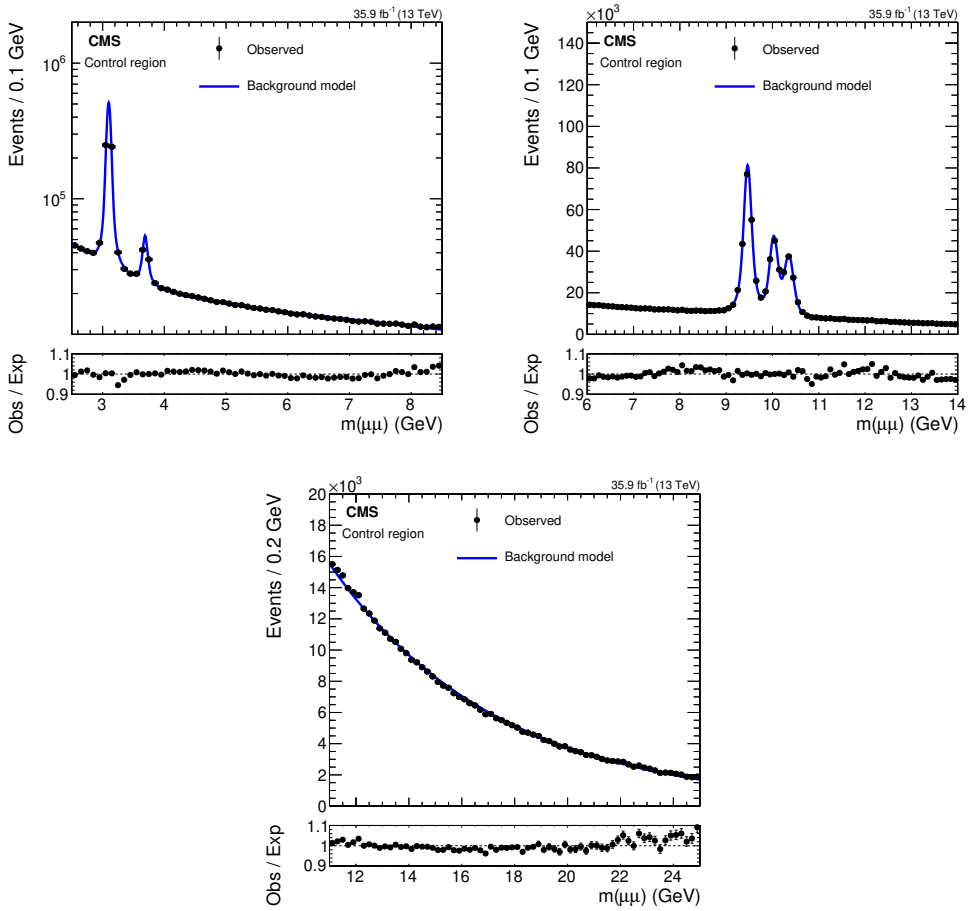


Figure 3. Background model fits and observed data in the control region $m(\mu\mu)$ distribution. The figures are divided into three fit ranges: $2.5 < m(\mu\mu) < 8.5\,\text{GeV}$ (upper left), $6 < m(\mu\mu) < 14\,\text{GeV}$ (upper right), and $11 < m(\mu\mu) < 25\,\text{GeV}$ (lower).

is 0.2–5.0%; most muons have $p_{\mathrm{T}} < 100\,\text{GeV}$ and thus an uncertainty of 0.2% [58]. For the τ_{h} reconstruction, there is an uncertainty in the τ_{h} identification efficiency of 5–18%, varying with $p_{\mathrm{T}}(\tau_{\mathrm{h}})$, and an uncertainty in the τ_{h} energy scale of 1.2–3.0% [63], varying with the number of charged and neutral hadrons in the τ_{h} decay.

The uncertainty in the luminosity normalization of simulated signal samples is 2.5% [66]. Uncertainty from pileup effects arises from the uncertainty of 4.6% [67] in the total inelastic cross section of pp interactions resulting in a 1% uncertainty in the signal yields. The efficiency correction for the rejection of jets tagged as originating from b quarks contributes an uncertainty of up to 3% in the signal yield.

As described in section 3, a correction to the simulated ggF signal samples to account for small differences in acceptance for the ggF and VBF H boson production modes contributes a 0.5% uncertainty in the signal yield. Theoretical uncertainties in the H boson production cross section are calculated by varying renormalization (μ_{R}) and factorization (μ_{F}) scales independently up and down by a factor of two with respect to the default values with the condition that $0.5 \leq \mu_{\mathrm{R}}/\mu_{\mathrm{F}} \leq 2$. The resulting uncertainties, combined with

JHEP08(2020)139

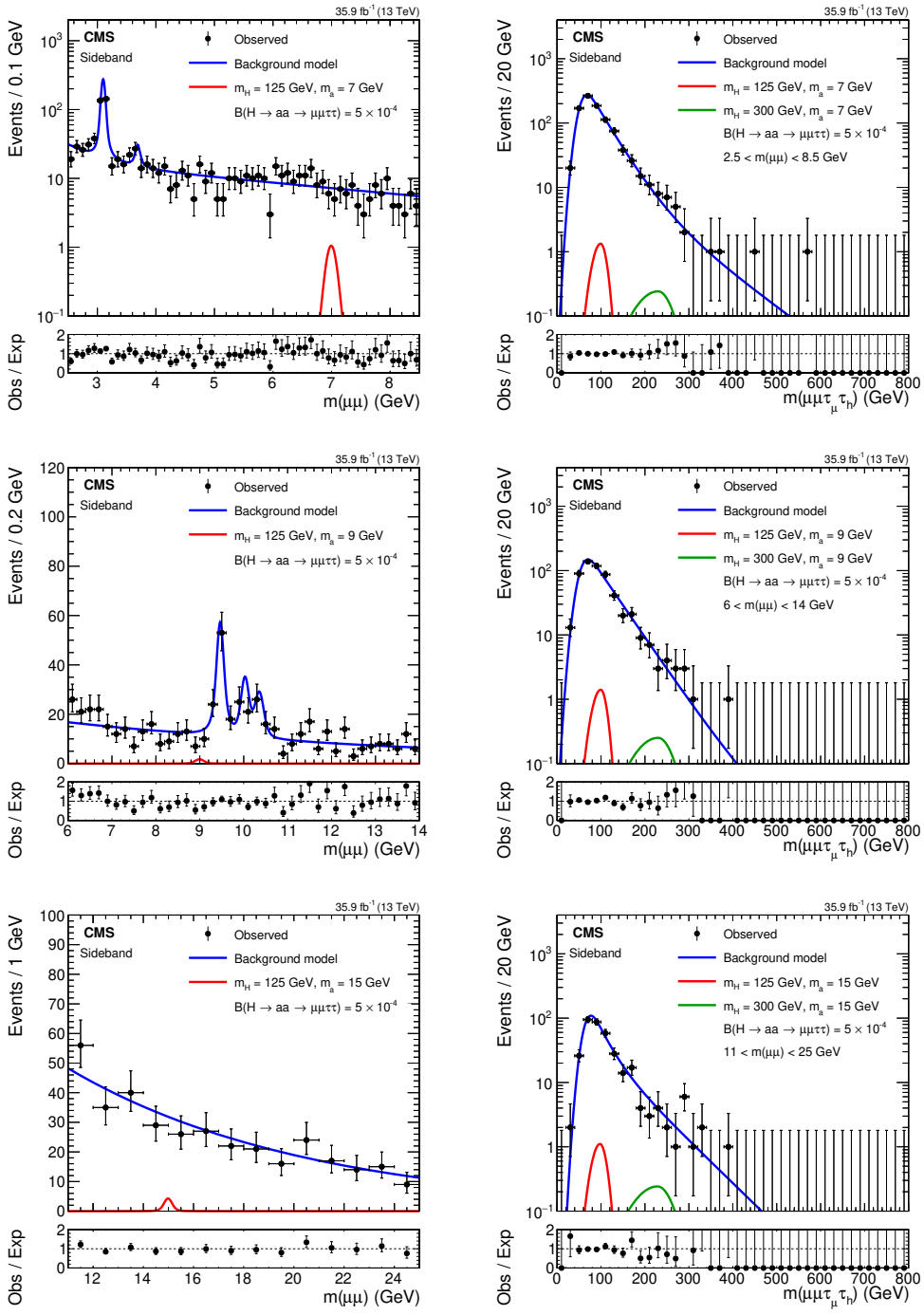


Figure 4. Projections of 2D background model fits and observed data in the sideband on the $m(\mu\mu)$ (left), and $m(\mu\mu\tau_\mu\tau_h)$ (right) axes with sample signal distributions that assume H boson masses of $m_H = 125$ and 300 GeV. The figures are divided into three fit ranges: $2.5 < m(\mu\mu) < 8.5$ GeV (upper), $6 < m(\mu\mu) < 14$ GeV (middle), and $11 < m(\mu\mu) < 25$ GeV (lower).

JHEP08(2020)139

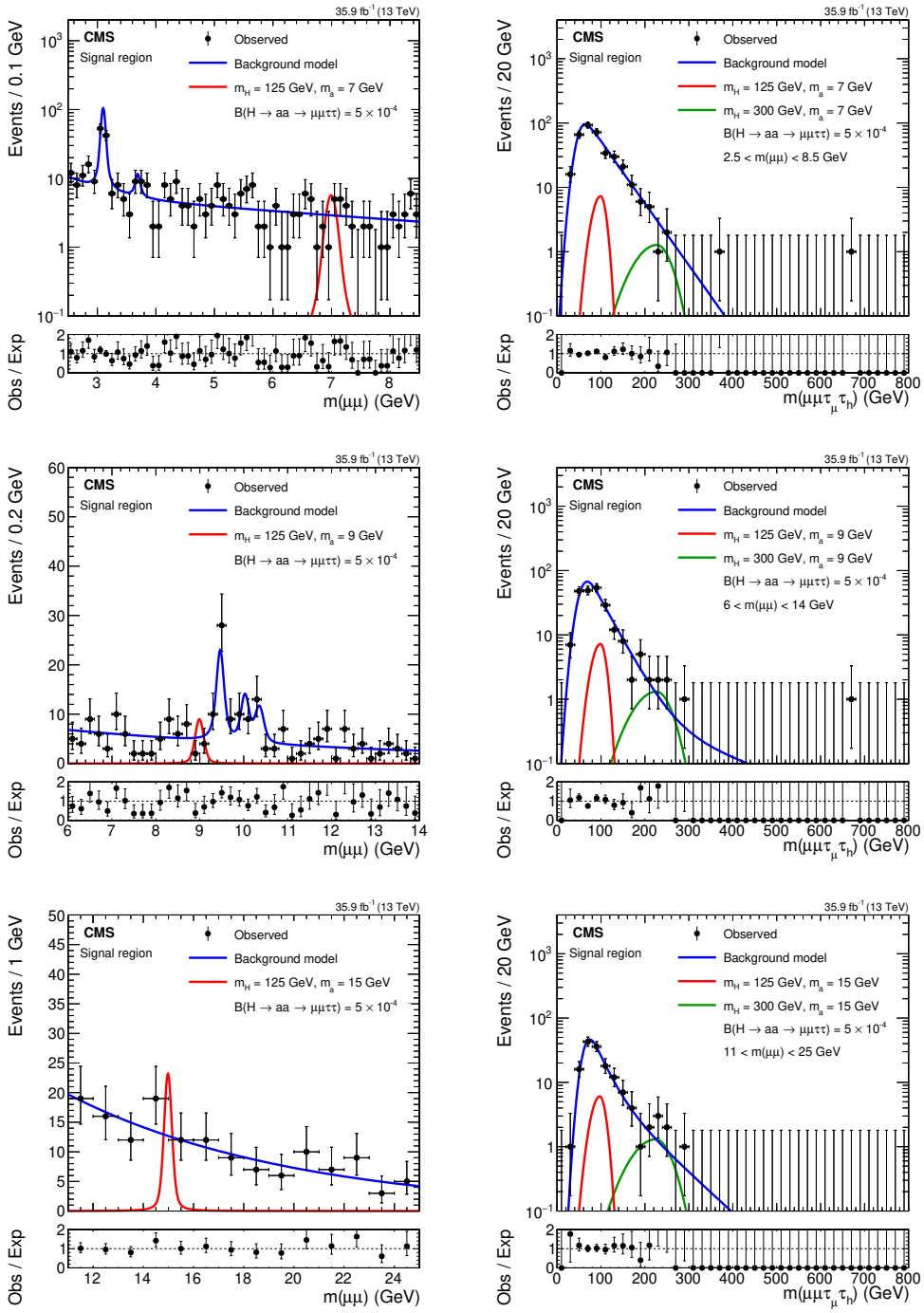


Figure 5. Projections of 2D background model fits and observed data in the signal region on the $m(\mu\mu)$ (left), and $m(\mu\mu\tau_\mu\tau_h)$ (right) axes with sample signal distributions that assume H boson masses of $m_H = 125$ and 300 GeV. The figures are divided into three fit ranges: $2.5 < m(\mu\mu) < 8.5$ GeV (upper), $6 < m(\mu\mu) < 14$ GeV (middle), and $11 < m(\mu\mu) < 25$ GeV (lower).

JHEP08(2020)139

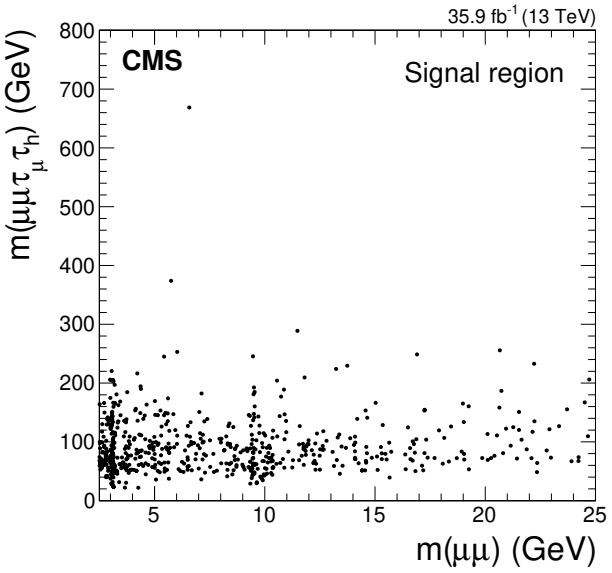


Figure 6. Observed data distribution, as a function of the 4-body visible mass and $\mu\mu$ invariant mass for the signal region; 614 events are observed.

those from ref. [46], contribute less than 1% to the overall signal yield uncertainty.

For the background model, the tight-to-loose method contributes a 15% uncertainty in the total expected yield in the signal region. This uncertainty arises from the application of the tight-to-loose ratio to the validation sideband to obtain a prediction for the model shapes in the validation region. The additional uncertainty in the relative normalizations of the low-mass meson resonances arises from differences in the tight-to-loose method predictions of the signal region distributions when derived from the sideband, as discussed in section 6. This uncertainty is measured to be 5–20% for $\psi(2S)$ and each Υ resonance, which yields up to a 3% uncertainty near these resonances in the final result.

8 Results

The observed distribution of data in the signal region is shown in figures 5 and 6. No significant excess of events is observed above the expected SM background. A modified frequentist approach based on the CL criterion [68, 69] is used for upper limit calculations [65] using the LHC test statistic [70]. Systematic uncertainties are represented as nuisance parameters assuming a log-normal PDF in the likelihood fit for uncertainties in the expected yields and a Gaussian PDF of uncertainties in the signal and background model parameters.

Model-independent upper limits at 95% CL are set on $\sigma_{\mathrm{H}}\mathcal{B}(\mathrm{H} \to \mathrm{aa} \to \mu\mu\tau\tau)/\sigma_{\mathrm{SM}}$ and are presented in figure 7. Here, σ_{SM} is the SM Higgs boson (or, for $m_{\mathrm{H}} = 300\,\mathrm{GeV}$, σ_{SM} is the SM-like Higgs boson) production cross section including ggF and VBF production modes [46]. Broadly, the sensitivity of this exclusion decreases at low values of m_{a} because of reconstruction inefficiencies as the decay products of the $\tau\tau$ pair overlap. In addition, for $m_{\mathrm{H}} = 125\,\mathrm{GeV}$, as m_{a} increases, the Lorentz boost decreases causing the products to be

JHEP08(2020)139

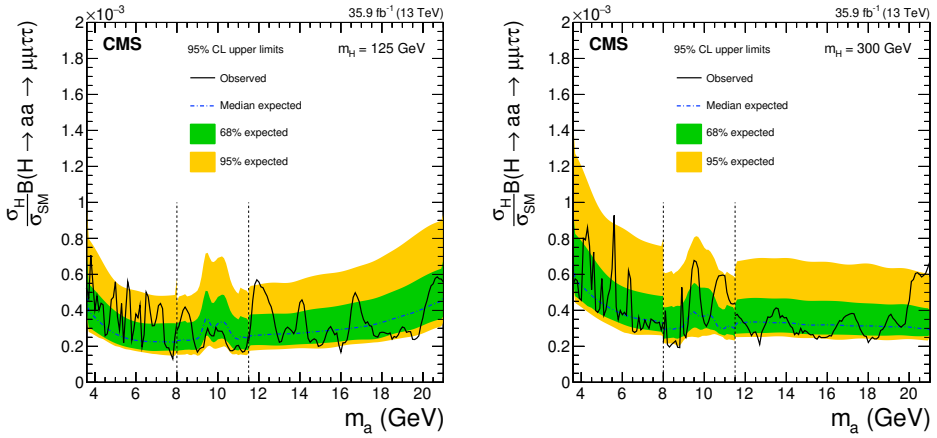


Figure 7. Model-independent 95% CL upper limits on $\sigma_{\mathrm{H}}\mathcal{B}(\mathrm{H} \to \mathrm{aa} \to \mu\mu\tau\tau)/\sigma_{\mathrm{SM}}$ as a function of pseudoscalar boson mass for a Higgs boson with $m_{\mathrm{H}} = 125\,\mathrm{GeV}$ (left), and 300 GeV (right). The vertical dashed lines indicate the transition between the $\mu\mu$ mass fit ranges for a given mass hypothesis, occurring at $m_{\mathrm{a}} = 8$ and 11.5 GeV. The inner (green) band and the outer (yellow) band indicate the regions containing 68 and 95%, respectively, of the distribution of limits expected under the background-only hypothesis.

well separated, failing the requirement of $\Delta R(\tau_\mu, \tau_{\mathrm{h}}) < 0.8$. The two peaking structures around $m_{\mathrm{a}} = 10\,\mathrm{GeV}$ are from the Υ resonances where the $\Upsilon(1\mathrm{S})$ resonance is resolvable but the $\Upsilon(2\mathrm{S})$ and $\Upsilon(3\mathrm{S})$ merge because the rejection power of the boosted $\tau_\mu\tau_{\mathrm{h}}$ selection sufficiently reduces the number of events in and around these peaks. A third peaking structure is not as apparent but is also present at the $\psi(2\mathrm{S})$ resonance. Comparison with an earlier $\sqrt{s} = 13\,\mathrm{TeV}$ result from the CMS Collaboration [40] targeting resolved $\tau\tau$ decay products is possible for SM Higgs boson decays with $15 < m_{\mathrm{a}} < 21\,\mathrm{GeV}$. In this case, the two approaches have similar sensitivity.

Upper limits on $\sigma_{\mathrm{H}}\mathcal{B}(\mathrm{H} \to \mathrm{aa})/\sigma_{\mathrm{SM}}$ for the 2HDM+S for each Type-I to -IV as a function of $\tan\beta$ and m_{a} are shown in figures 8 and 9. The assumed model branching fractions for pseudoscalar decays to $\mu\mu$ and $\tau\tau$ are taken from ref. [71], and the branching fraction $\mathcal{B}(\mathrm{aa} \to \mu\mu\tau\tau)$ depends strongly on the 2HDM+S type [7]. The branching fractions are calculated in $\tan\beta$ increments of 0.5 above $\tan\beta = 1$ and increments of 0.1 below, and a linear interpolation is applied between the calculated points in figure 9. For the Type-I and -II models, we primarily probe the $2m_\tau < m_{\mathrm{a}} < 2m_{\mathrm{b}}$ range, with the Type-I upper limits approximately independent of $\tan\beta$. In the Type-I model, the most stringent limit of 5% is set for $m_{\mathrm{a}} \approx 4.5\,\mathrm{GeV}$. In the Type-III model, this analysis has exclusion power over the full pseudoscalar mass range probed, especially at large $\tan\beta$. For the Type-II and -III models with m_{a} below the $\mathrm{b\bar{b}}$ threshold, upper limits on $\mathcal{B}(\mathrm{H} \to \mathrm{aa})$ are stronger than the 0.47 inferred from combined measurements of SM Higgs couplings [9] for $\tan\beta \gtrsim 0.8$-0.9, becoming as strong as 10% for $\tan\beta \gtrsim 1.5$. In the Type-III models, strong upper limits are set for all pseudoscalar boson masses tested when $\tan\beta \gtrsim 1.5$. The Type-IV model, however, can only be effectively probed in the low-$\tan\beta$ region. For a given m_{a}, the ratio of decay rates to $\mu\mu$ and $\tau\tau$, respectively $\mathcal{B}(\mathrm{a} \to \mu\mu)$ and $\mathcal{B}(\mathrm{a} \to \tau\tau)$,

JHEP08(2020)139

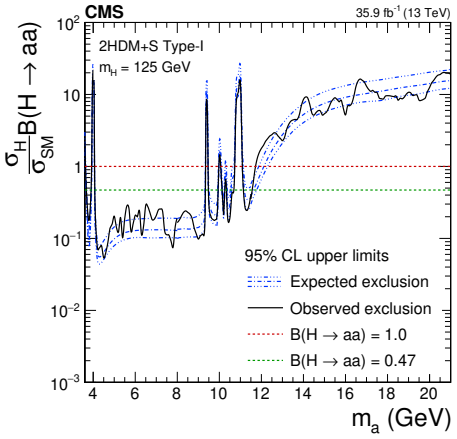


Figure 8. Observed (black) and expected (blue, median and 68%) model-specific 95% CL upper limits on $\sigma_{\mathrm{H}}\mathcal{B}(\mathrm{H} \to \mathrm{aa})/\sigma_{\mathrm{SM}}$ as a function of m_{a} for the Type-I 2HDM+S at $\tan\beta = 1.5$ and $m_{\mathrm{H}} = 125\,\mathrm{GeV}$. The assumed model branching fractions for pseudoscalar Higgs boson decay to $\mu\mu$ and $\tau\tau$ are taken from ref. [71] and are approximately independent of $\tan\beta$.

depends only on m_μ and m_τ [7, 71]. Thus, these results can be converted into upper limits on $\sigma_{\mathrm{H}}\mathcal{B}(\mathrm{H} \to \mathrm{aa})/\sigma_{\mathrm{SM}}$. Contours for different $\mathcal{B}(\mathrm{H} \to \mathrm{aa})$ values are overlaid. Compared with an earlier result by CMS [40], these upper limits are more stringent (where they can be compared) and extend to lower values of m_{a}.

9 Summary

A search for Higgs boson (H) decays to a pair of light pseudoscalar bosons (a) is presented, including the first such LHC results for an H with mass above 125 GeV. The light pseudoscalars decay to $\mu\mu$ and $\tau\tau$ with substantial overlap between the leptons because of the Lorentz boost. This difficult topology motivates the development of a dedicated $\tau_\mu\tau_{\mathrm{h}}$ reconstruction method to increase the acceptance. Data collected by the CMS Collaboration at $\sqrt{s} = 13\,\mathrm{TeV}$, corresponding to an integrated luminosity of $35.9\,\mathrm{fb}^{-1}$, are examined and no significant excess over standard model (SM) processes is observed. This analysis obtains model-independent upper limits at 95% confidence level on the branching fraction ($\mathcal{B}$) of a SM-like Higgs boson (H), decaying to a pair of pseudoscalar bosons (a) in the $\mu\mu\tau\tau$ final state, $\sigma_{\mathrm{H}}\mathcal{B}(\mathrm{H} \to \mathrm{aa} \to \mu\mu\tau\tau)/\sigma_{\mathrm{SM}}$, as well as model-specific upper limits on $\sigma_{\mathrm{H}}\mathcal{B}(\mathrm{H} \to \mathrm{aa})/\sigma_{\mathrm{SM}}$ for Type-I, -II, -III, and -IV two Higgs doublets plus singlet models. In the Type-I model, the upper limit on the allowed branching fraction is approximately independent of $\tan\beta$, with the most stringent limit of 5% set for $m_{\mathrm{a}} \approx 4.5\,\mathrm{GeV}$. For the Type-II and -III models with m_{a} below the $\mathrm{b\bar{b}}$ threshold, upper limits on $\mathcal{B}(\mathrm{H} \to \mathrm{aa})$ are stronger than the 0.47 inferred from combined measurements of SM Higgs couplings for $\tan\beta \gtrsim 0.8$-0.9, becoming as strong as 10% for $\tan\beta \gtrsim 1.5$. In the Type-III models, the predicted branching fraction to leptons increases with $\tan\beta$, leading to strong upper limits for all pseudoscalar boson masses tested when $\tan\beta \gtrsim 1.5$. In contrast, the strongest upper limits for Type-IV models are set when $\tan\beta < 1$. These results significantly extend upper limits obtained by earlier searches by the CMS and ATLAS Collaborations, such as those

JHEP08(2020)139

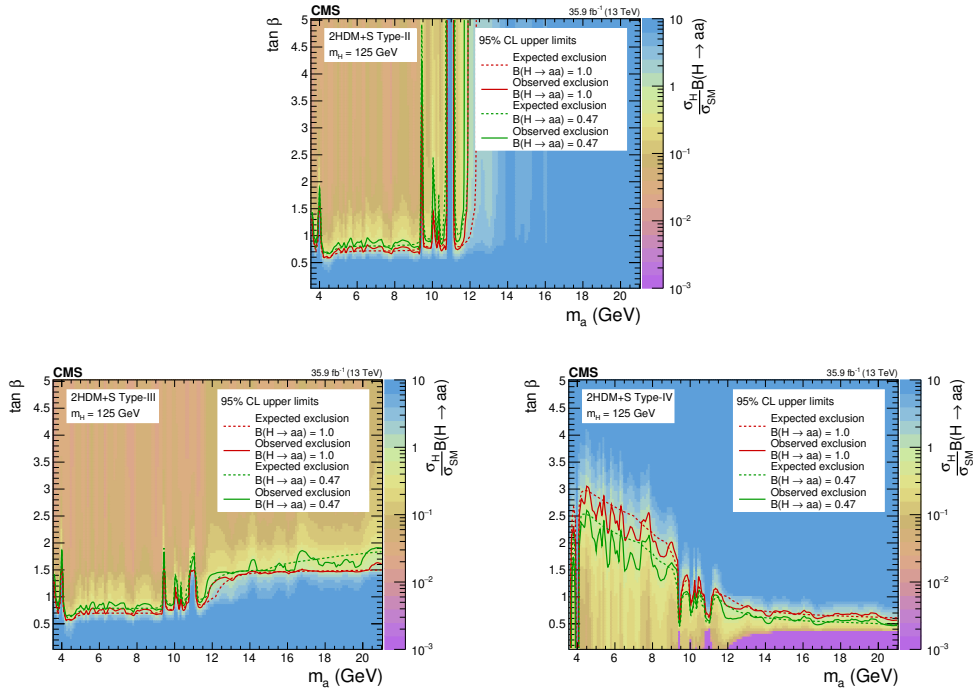


Figure 9. Model-specific 95% CL upper limits on $\sigma_{\mathrm{H}}\mathcal{B}(\mathrm{H} \to \mathrm{aa})/\sigma_{\mathrm{SM}}$ for three model types of the 2HDM+S as a function of $\tan\beta$ and m_{a}, for $m_{\mathrm{H}} = 125\,\mathrm{GeV}$. Contours for two values of $\mathcal{B}(\mathrm{H} \to \mathrm{aa})$ are shown for reference. The assumed model branching fractions for pseudoscalar Higgs boson decay to $\mu\mu$ and $\tau\tau$ are taken from ref. [71].

obtained by CMS with 8 TeV data [39], and are complementary to present searches (e.g. ref. [40]) at higher m_{a} that lead to resolved $\mu\mu$ and $\tau\tau$ final states.

Acknowledgments

We congratulate our colleagues in the CERN accelerator departments for the excellent performance of the LHC and thank the technical and administrative staffs at CERN and at other CMS institutes for their contributions to the success of the CMS effort. In addition, we gratefully acknowledge the computing centers and personnel of the Worldwide LHC Computing Grid for delivering so effectively the computing infrastructure essential to our analyses. Finally, we acknowledge the enduring support for the construction and operation of the LHC and the CMS detector provided by the following funding agencies: BMBWF and FWF (Austria); FNRS and FWO (Belgium); CNPq, CAPES, FAPERJ, FAPERGS, and FAPESP (Brazil); MES (Bulgaria); CERN; CAS, MoST, and NSFC (China); COLCIENCIAS (Colombia); MSES and CSF (Croatia); RPF (Cyprus); SENESCYT (Ecuador); MoER, ERC IUT, PUT and ERDF (Estonia); Academy of Finland, MEC, and HIP (Finland); CEA and CNRS/IN2P3 (France); BMBF, DFG, and HGF (Germany); GSRT (Greece); NKFIA (Hungary); DAE and DST (India); IPM (Iran); SFI (Ireland); INFN (Italy); MSIP and NRF (Republic of Korea); MES (Latvia); LAS (Lithuania); MOE and UM (Malaysia); BUAP, CINVESTAV, CONACYT, LNS, SEP, and UASLP-FAI (Mexico);

JHEP08(2020)139

MOS (Montenegro); MBIE (New Zealand); PAEC (Pakistan); MSHE and NSC (Poland); FCT (Portugal); JINR (Dubna); MON, RosAtom, RAS, RFBR, and NRC KI (Russia); MESTD (Serbia); SEIDI, CPAN, PCTI, and FEDER (Spain); MOSTR (Sri Lanka); Swiss Funding Agencies (Switzerland); MST (Taipei); ThEPCenter, IPST, STAR, and NSTDA (Thailand); TUBITAK and TAEK (Turkey); NASU (Ukraine); STFC (United Kingdom); DOE and NSF (U.S.A.).

Individuals have received support from the Marie-Curie program and the European Research Council and Horizon 2020 Grant, contract Nos. 675440, 752730, and 765710 (European Union); the Leventis Foundation; the A.P. Sloan Foundation; the Alexander von Humboldt Foundation; the Belgian Federal Science Policy Office; the Fonds pour la Formation à la Recherche dans l'Industrie et dans l'Agriculture (FRIA-Belgium); the Agentschap voor Innovatie door Wetenschap en Technologie (IWT-Belgium); the F.R.S.-FNRS and FWO (Belgium) under the "Excellence of Science — EOS" — be.h project n. 30820817; the Beijing Municipal Science & Technology Commission, No. Z191100007219010; the Ministry of Education, Youth and Sports (MEYS) of the Czech Republic; the Deutsche Forschungsgemeinschaft (DFG) under Germany's Excellence Strategy — EXC 2121 "Quantum Universe" — 390833306; the Lendület ("Momentum") Program and the János Bolyai Research Scholarship of the Hungarian Academy of Sciences, the New National Excellence Program ÚNKP, the NKFIA research grants 123842, 123959, 124845, 124850, 125105, 128713, 128786, and 129058 (Hungary); the Council of Science and Industrial Research, India; the HOMING PLUS program of the Foundation for Polish Science, cofinanced from European Union, Regional Development Fund, the Mobility Plus program of the Ministry of Science and Higher Education, the National Science Center (Poland), contracts Harmonia 2014/14/M/ST2/00428, Opus 2014/13/B/ST2/02543, 2014/15/B/ST2/03998, and 2015/19/B/ST2/02861, Sonata-bis 2012/07/E/ST2/01406; the National Priorities Research Program by Qatar National Research Fund; the Ministry of Science and Education, grant no. 14.W03.31.0026 (Russia); the Tomsk Polytechnic University Competitiveness Enhancement Program and "Nauka" Project FSWW-2020-0008 (Russia); the Programa Estatal de Fomento de la Investigación Científica y Técnica de Excelencia María de Maeztu, grant MDM-2015-0509 and the Programa Severo Ochoa del Principado de Asturias; the Thalis and Aristeia programs cofinanced by EU-ESF and the Greek NSRF; the Rachadapisek Sompot Fund for Postdoctoral Fellowship, Chulalongkorn University and the Chulalongkorn Academic into Its 2nd Century Project Advancement Project (Thailand); the Kavli Foundation; the Nvidia Corporation; the SuperMicro Corporation; the Welch Foundation, contract C-1845; and the Weston Havens Foundation (U.S.A.).

Open Access. This article is distributed under the terms of the Creative Commons Attribution License (CC-BY 4.0), which permits any use, distribution and reproduction in any medium, provided the original author(s) and source are credited.

References

[1] ATLAS collaboration, *Measurements of Higgs boson production and couplings in diboson final states with the ATLAS detector at the LHC*, *Phys. Lett. B* **726** (2013) 88 [*Erratum ibid.* **734** (2014) 406] [arXiv:1307.1427] [INSPIRE].

JHEP08(2020)139

[2] ATLAS and CMS collaborations, *Measurements of the Higgs boson production and decay rates and constraints on its couplings from a combined ATLAS and CMS analysis of the LHC pp collision data at $\sqrt{s} = 7$ and 8 TeV*, *JHEP* **08** (2016) 045 [arXiv:1606.02266] [INSPIRE].

[3] CMS collaboration, *Measurements of properties of the Higgs boson decaying into the four-lepton final state in pp collisions at $\sqrt{s} = 13$ TeV*, *JHEP* **11** (2017) 047 [arXiv:1706.09936] [INSPIRE].

[4] ATLAS collaboration, *Measurement of the Higgs boson mass from the $H \to \gamma\gamma$ and $H \to ZZ^* \to 4\ell$ channels with the ATLAS detector using 25 fb^{-1} of pp collision data*, *Phys. Rev. D* **90** (2014) 052004 [arXiv:1406.3827] [INSPIRE].

[5] ATLAS and CMS collaborations, *Combined measurement of the Higgs boson mass in pp collisions at $\sqrt{s} = 7$ and 8 TeV with the ATLAS and CMS experiments*, *Phys. Rev. Lett.* **114** (2015) 191803 [arXiv:1503.07589] [INSPIRE].

[6] G.C. Branco, P.M. Ferreira, L. Lavoura, M.N. Rebelo, M. Sher and J.P. Silva, *Theory and phenomenology of two-Higgs-doublet models*, *Phys. Rept.* **516** (2012) 1 [arXiv:1106.0034] [INSPIRE].

[7] D. Curtin et al., *Exotic decays of the 125 GeV Higgs boson*, *Phys. Rev. D* **90** (2014) 075004 [arXiv:1312.4992] [INSPIRE].

[8] U. Ellwanger, C. Hugonie and A.M. Teixeira, *The next-to-minimal supersymmetric standard model*, *Phys. Rept.* **496** (2010) 1 [arXiv:0910.1785] [INSPIRE].

[9] CMS collaboration, *Combined measurements of Higgs boson couplings in proton-proton collisions at $\sqrt{s} = 13$ TeV*, *Eur. Phys. J. C* **79** (2019) 421 [arXiv:1809.10733] [INSPIRE].

[10] R. Dermisek and J.F. Gunion, *Escaping the large fine tuning and little hierarchy problems in the next to minimal supersymmetric model and $h \to aa$ decays*, *Phys. Rev. Lett.* **95** (2005) 041801 [hep-ph/0502105] [INSPIRE].

[11] R. Dermisek and J.F. Gunion, *The NMSSM close to the R-symmetry limit and naturalness in $h \to aa$ decays for $m(a) < 2m(b)$*, *Phys. Rev. D* **75** (2007) 075019 [hep-ph/0611142] [INSPIRE].

[12] S. Chang, R. Dermisek, J.F. Gunion and N. Weiner, *Nonstandard Higgs boson decays*, *Ann. Rev. Nucl. Part. Sci.* **58** (2008) 75 [arXiv:0801.4554] [INSPIRE].

[13] J.F. Gunion, H.E. Haber, G.L. Kane and S. Dawson, *The Higgs Hunter's guide*, Frontiers in Physics volume 80. Perseus Books, U.S.A. (2000).

[14] S.F. King, M. Mühlleitner, R. Nevzorov and K. Walz, *Natural NMSSM Higgs bosons*, *Nucl. Phys. B* **870** (2013) 323 [arXiv:1211.5074] [INSPIRE].

[15] A. Celis, V. Ilisie and A. Pich, *LHC constraints on two-Higgs doublet models*, *JHEP* **07** (2013) 053 [arXiv:1302.4022] [INSPIRE].

[16] B. Grinstein and P. Uttayarat, *Carving out parameter space in type-II two Higgs doublets model*, *JHEP* **06** (2013) 094 [*Erratum ibid.* **09** (2013) 110] [arXiv:1304.0028] [INSPIRE].

[17] B. Coleppa, F. Kling and S. Su, *Constraining type II 2HDM in light of LHC Higgs searches*, *JHEP* **01** (2014) 161 [arXiv:1305.0002] [INSPIRE].

[18] C.-Y. Chen, S. Dawson and M. Sher, *Heavy Higgs searches and constraints on two Higgs doublet models*, *Phys. Rev. D* **88** (2013) 015018 [*Erratum ibid.* **88** (2013) 039901] [arXiv:1305.1624] [INSPIRE].

JHEP08(2020)139

[19] N. Craig, J. Galloway and S. Thomas, *Searching for signs of the second Higgs doublet*, arXiv:1305.2424 [INSPIRE].

[20] L. Wang and X.-F. Han, *Status of the aligned two-Higgs-doublet model confronted with the Higgs data*, *JHEP* **04** (2014) 128 [arXiv:1312.4759] [INSPIRE].

[21] J. Cao, F. Ding, C. Han, J.M. Yang and J. Zhu, *A light Higgs scalar in the NMSSM confronted with the latest LHC Higgs data*, *JHEP* **11** (2013) 018 [arXiv:1309.4939] [INSPIRE].

[22] N.D. Christensen, T. Han, Z. Liu and S. Su, *Low-mass Higgs bosons in the NMSSM and their LHC implications*, *JHEP* **08** (2013) 019 [arXiv:1303.2113] [INSPIRE].

[23] D.G. Cerdeno, P. Ghosh and C.B. Park, *Probing the two light Higgs scenario in the NMSSM with a low-mass pseudoscalar*, *JHEP* **06** (2013) 031 [arXiv:1301.1325] [INSPIRE].

[24] G. Chalons and F. Domingo, *Analysis of the Higgs potentials for two doublets and a singlet*, *Phys. Rev. D* **86** (2012) 115024 [arXiv:1209.6235] [INSPIRE].

[25] A. Ahriche, A. Arhrib and S. Nasri, *Higgs phenomenology in the two-singlet model*, *JHEP* **02** (2014) 042 [arXiv:1309.5615] [INSPIRE].

[26] J. Baglio, O. Eberhardt, U. Nierste and M. Wiebusch, *Benchmarks for Higgs pair production and heavy Higgs boson searches in the two-Higgs-doublet model of type II*, *Phys. Rev. D* **90** (2014) 015008 [arXiv:1403.1264] [INSPIRE].

[27] B. Dumont, J.F. Gunion, Y. Jiang and S. Kraml, *Constraints on and future prospects for two-Higgs-doublet models in light of the LHC Higgs signal*, *Phys. Rev. D* **90** (2014) 035021 [arXiv:1405.3584] [INSPIRE].

[28] J. Bernon, J.F. Gunion, H.E. Haber, Y. Jiang and S. Kraml, *Scrutinizing the alignment limit in two-Higgs-doublet models: $m_h = 125$ GeV*, *Phys. Rev. D* **92** (2015) 075004 [arXiv:1507.00933] [INSPIRE].

[29] ALEPH collaboration, *Search for a nonminimal Higgs boson produced in the reaction $e^+e^- \to hZ^*$*, *Phys. Lett. B* **313** (1993) 312 [INSPIRE].

[30] L3 collaboration, *Search for neutral Higgs boson production through the process $e^+e^- \to Z^*H^0$*, *Phys. Lett. B* **385** (1996) 454 [INSPIRE].

[31] OPAL collaboration, *Decay mode independent searches for new scalar bosons with the OPAL detector at LEP*, *Eur. Phys. J. C* **27** (2003) 311 [hep-ex/0206022] [INSPIRE].

[32] S.F. King, M. Mühlleitner, R. Nevzorov and K. Walz, *Discovery prospects for NMSSM Higgs bosons at the high-energy Large Hadron Collider*, *Phys. Rev. D* **90** (2014) 095014 [arXiv:1408.1120] [INSPIRE].

[33] ALEPH collaboration, *Search for neutral Higgs bosons decaying into four taus at LEP2*, *JHEP* **05** (2010) 049 [arXiv:1003.0705] [INSPIRE].

[34] CMS collaboration, *Search for a light pseudoscalar Higgs boson in the dimuon decay channel in pp collisions at $\sqrt{s} = 7$ TeV*, *Phys. Rev. Lett.* **109** (2012) 121801 [arXiv:1206.6326] [INSPIRE].

[35] R. Dermisek and J.F. Gunion, *Direct production of a light CP-odd Higgs boson at the Tevatron and LHC*, *Phys. Rev. D* **81** (2010) 055001 [arXiv:0911.2460] [INSPIRE].

[36] LHCb collaboration, *Search for a dimuon resonance in the Υ mass region*, *JHEP* **09** (2018) 147 [arXiv:1805.09820] [INSPIRE].

JHEP08(2020)139

[37] CMS collaboration, *A search for pair production of new light bosons decaying into muons in proton-proton collisions at* 13 *TeV*, *Phys. Lett. B* **796** (2019) 131 [arXiv:1812.00380] [INSPIRE].

[38] ATLAS collaboration, *Search for Higgs boson decays to beyond-the-Standard-Model light bosons in four-lepton events with the ATLAS detector at* $\sqrt{s} = 13$ *TeV*, *JHEP* **06** (2018) 166 [arXiv:1802.03388] [INSPIRE].

[39] CMS collaboration, *Search for light bosons in decays of the* 125 *GeV Higgs boson in proton-proton collisions at* $\sqrt{s} = 8$ *TeV*, *JHEP* **10** (2017) 076 [arXiv:1701.02032] [INSPIRE].

[40] CMS collaboration, *Search for an exotic decay of the Higgs boson to a pair of light pseudoscalars in the final state of two muons and two* τ *leptons in proton-proton collisions at* $\sqrt{s} = 13$ *TeV*, *JHEP* **11** (2018) 018 [arXiv:1805.04865] [INSPIRE].

[41] CMS collaboration, *Search for an exotic decay of the Higgs boson to a pair of light pseudoscalars in the final state with two b quarks and two* τ *leptons in proton-proton collisions at* $\sqrt{s} = 13$ *TeV*, *Phys. Lett. B* **785** (2018) 462 [arXiv:1805.10191] [INSPIRE].

[42] CMS collaboration, *Search for light pseudoscalar boson pairs produced from decays of the* 125 *GeV Higgs boson in final states with two muons and two nearby tracks in pp collisions at* $\sqrt{s} = 13$ *TeV*, *Phys. Lett. B* **800** (2020) 135087 [arXiv:1907.07235] [INSPIRE].

[43] ATLAS collaboration, *Search for Higgs bosons decaying to aa in the* $\mu\mu\tau\tau$ *final state in pp collisions at* $\sqrt{s} = 8$ *TeV with the ATLAS experiment*, *Phys. Rev. D* **92** (2015) 052002 [arXiv:1505.01609] [INSPIRE].

[44] ATLAS collaboration, *Search for Higgs boson decays into a pair of light bosons in the* $bb\mu\mu$ *final state in pp collision at* $\sqrt{s} = 13$ *TeV with the ATLAS detector*, *Phys. Lett. B* **790** (2019) 1 [arXiv:1807.00539] [INSPIRE].

[45] ATLAS collaboration, *Search for the Higgs boson produced in association with a vector boson and decaying into two spin-zero particles in the* $H \to aa \to 4b$ *channel in pp collisions at* $\sqrt{s} = 13$ *TeV with the ATLAS detector*, *JHEP* **10** (2018) 031 [arXiv:1806.07355] [INSPIRE].

[46] LHC Higgs Cross Section Working Group, *Handbook of LHC Higgs cross sections: 4. deciphering the nature of the Higgs sector*, arXiv:1610.07922 [INSPIRE].

[47] J. Bernon, J.F. Gunion, Y. Jiang and S. Kraml, *Light Higgs bosons in two-Higgs-doublet models*, *Phys. Rev. D* **91** (2015) 075019 [arXiv:1412.3385] [INSPIRE].

[48] CMS collaboration, *The CMS trigger system*, 2017 *JINST* **12** P01020 [arXiv:1609.02366] [INSPIRE].

[49] CMS collaboration, *The CMS experiment at the CERN LHC*, 2008 *JINST* **3** S08004 [INSPIRE].

[50] J. Alwall et al., *The automated computation of tree-level and next-to-leading order differential cross sections, and their matching to parton shower simulations*, *JHEP* **07** (2014) 079 [arXiv:1405.0301] [INSPIRE].

[51] T. Sjöstrand et al., *An introduction to PYTHIA 8.2*, *Comput. Phys. Commun.* **191** (2015) 159 [arXiv:1410.3012] [INSPIRE].

[52] CMS collaboration, *Event generator tunes obtained from underlying event and multiparton scattering measurements*, *Eur. Phys. J. C* **76** (2016) 155 [arXiv:1512.00815] [INSPIRE].

JHEP08(2020)139

[53] NNPDF collaboration, *Parton distributions from high-precision collider data*, *Eur. Phys. J. C* **77** (2017) 663 [arXiv:1706.00428] [INSPIRE].

[54] GEANT4 collaboration, *GEANT4 — A simulation toolkit*, *Nucl. Instrum. Meth. A* **506** (2003) 250 [INSPIRE].

[55] CMS collaboration, *Particle-flow reconstruction and global event description with the CMS detector*, 2017 *JINST* **12** P10003 [arXiv:1706.04965] [INSPIRE].

[56] M. Cacciari, G.P. Salam and G. Soyez, *The anti-k_t jet clustering algorithm*, *JHEP* **04** (2008) 063 [arXiv:0802.1189] [INSPIRE].

[57] M. Cacciari, G.P. Salam and G. Soyez, *FastJet user manual*, *Eur. Phys. J. C* **72** (2012) 1896 [arXiv:1111.6097] [INSPIRE].

[58] CMS collaboration, *Performance of the CMS muon detector and muon reconstruction with proton-proton collisions at $\sqrt{s} = 13$ TeV*, 2018 *JINST* **13** P06015 [arXiv:1804.04528] [INSPIRE].

[59] CMS collaboration, *Determination of jet energy calibration and transverse momentum resolution in CMS*, 2011 *JINST* **6** P11002 [arXiv:1107.4277] [INSPIRE].

[60] CMS collaboration, *Pileup mitigation at CMS in 13 TeV data*, CMS-PAS-JME-18-001 (2019).

[61] CMS collaboration, *Identification of b-quark jets with the CMS experiment*, 2013 *JINST* **8** P04013 [arXiv:1211.4462] [INSPIRE].

[62] CMS collaboration, *Identification of heavy-flavour jets with the CMS detector in pp collisions at 13 TeV*, 2018 *JINST* **13** P05011 [arXiv:1712.07158] [INSPIRE].

[63] CMS collaboration, *Performance of reconstruction and identification of τ leptons decaying to hadrons and ν_τ in pp collisions at $\sqrt{s} = 13$ TeV*, 2018 *JINST* **13** P10005 [arXiv:1809.02816] [INSPIRE].

[64] CMS collaboration, *Measurement of the inclusive W and Z production cross sections in pp collisions at $\sqrt{s} = 7$ TeV*, *JHEP* **10** (2011) 132 [arXiv:1107.4789] [INSPIRE].

[65] Particle Data Group, *Review of particle physics*, *Phys. Rev. D* **98** (2018) 030001 [INSPIRE].

[66] CMS collaboration, *CMS luminosity measurements for the 2016 data taking period*, CMS-PAS-LUM-17-001 (2017).

[67] CMS collaboration, *Measurement of the inelastic proton-proton cross section at $\sqrt{s} = 13$ TeV*, *JHEP* **07** (2018) 161 [arXiv:1802.02613] [INSPIRE].

[68] T. Junk, *Confidence level computation for combining searches with small statistics*, *Nucl. Instrum. Meth. A* **434** (1999) 435 [hep-ex/9902006] [INSPIRE].

[69] A.L. Read, *Presentation of search results: the CL_s technique*, *J. Phys. G* **28** (2002) 2693 [INSPIRE].

[70] ATLAS collaboration, CMS collaboration and LHC Higgs Combination Group, *Procedure for the LHC Higgs boson search combination in Summer 2011*, CMS-NOTE-2011-005 (2011) [ATL-PHYS-PUB-2011-11].

[71] U. Haisch, J.F. Kamenik, A. Malinauskas and M. Spira, *Collider constraints on light pseudoscalars*, *JHEP* **03** (2018) 178 [arXiv:1802.02156] [INSPIRE].

JHEP08(2020)139

The CMS collaboration

Yerevan Physics Institute, Yerevan, Armenia

A.M. Sirunyan[†], A. Tumasyan

Institut für Hochenergiephysik, Wien, Austria

W. Adam, F. Ambrogi, T. Bergauer, M. Dragicevic, J. Erö, A. Escalante Del Valle, R. Frühwirth[1], M. Jeitler[1], N. Krammer, L. Lechner, D. Liko, T. Madlener, I. Mikulec, N. Rad, J. Schieck[1], R. Schöfbeck, M. Spanring, S. Templ, W. Waltenberger, C.-E. Wulz[1], M. Zarucki

Institute for Nuclear Problems, Minsk, Belarus

V. Chekhovsky, A. Litomin, V. Makarenko, J. Suarez Gonzalez

Universiteit Antwerpen, Antwerpen, Belgium

M.R. Darwish[2], E.A. De Wolf, D. Di Croce, X. Janssen, T. Kello[3], A. Lelek, M. Pieters, H. Rejeb Sfar, H. Van Haevermaet, P. Van Mechelen, S. Van Putte, N. Van Remortel

Vrije Universiteit Brussel, Brussel, Belgium

F. Blekman, E.S. Bols, S.S. Chhibra, J. D'Hondt, J. De Clercq, D. Lontkovskyi, S. Lowette, I. Marchesini, S. Moortgat, Q. Python, S. Tavernier, W. Van Doninck, P. Van Mulders

Université Libre de Bruxelles, Bruxelles, Belgium

D. Beghin, B. Bilin, B. Clerbaux, G. De Lentdecker, H. Delannoy, B. Dorney, L. Favart, A. Grebenyuk, A.K. Kalsi, I. Makarenko, L. Moureaux, L. Pétré, A. Popov, N. Postiau, E. Starling, L. Thomas, C. Vander Velde, P. Vanlaer, D. Vannerom, L. Wezenbeek

Ghent University, Ghent, Belgium

T. Cornelis, D. Dobur, I. Khvastunov[4], M. Niedziela, C. Roskas, K. Skovpen, M. Tytgat, W. Verbeke, B. Vermassen, M. Vit

Université Catholique de Louvain, Louvain-la-Neuve, Belgium

G. Bruno, F. Bury, C. Caputo, P. David, C. Delaere, M. Delcourt, I.S. Donertas, A. Giammanco, V. Lemaitre, J. Prisciandaro, A. Saggio, A. Taliercio, M. Teklishyn, P. Vischia, S. Wuyckens, J. Zobec

Centro Brasileiro de Pesquisas Fisicas, Rio de Janeiro, Brazil

G.A. Alves, G. Correia Silva, C. Hensel, A. Moraes

Universidade do Estado do Rio de Janeiro, Rio de Janeiro, Brazil

W.L. Aldá Júnior, E. Belchior Batista Das Chagas, W. Carvalho, J. Chinellato[5], E. Coelho, E.M. Da Costa, G.G. Da Silveira[6], D. De Jesus Damiao, S. Fonseca De Souza, H. Malbouisson, J. Martins[7], D. Matos Figueiredo, M. Medina Jaime[8], M. Melo De Almeida, C. Mora Herrera, L. Mundim, H. Nogima, P. Rebello Teles, L.J. Sanchez Rosas, A. Santoro, S.M. Silva Do Amaral, A. Sznajder, M. Thiel, E.J. Tonelli Manganote[5], F. Torres Da Silva De Araujo, A. Vilela Pereira

JHEP08(2020)139

Universidade Estadual Paulista[a], Universidade Federal do ABC[b], São Paulo, Brazil
C.A. Bernardes[a], L. Calligaris[a], T.R. Fernandez Perez Tomei[a], E.M. Gregores[b], D.S. Lemos, P.G. Mercadante[b], S.F. Novaes[a], SandraS. Padula[a]

Institute for Nuclear Research and Nuclear Energy, Bulgarian Academy of Sciences, Sofia, Bulgaria
A. Aleksandrov, G. Antchev, I. Atanasov, R. Hadjiiska, P. Iaydjiev, M. Misheva, M. Rodozov, M. Shopova, G. Sultanov

University of Sofia, Sofia, Bulgaria
M. Bonchev, A. Dimitrov, T. Ivanov, L. Litov, B. Pavlov, P. Petkov, A. Petrov

Beihang University, Beijing, China
W. Fang[3], X. Gao[3], Q. Guo, H. Wang, L. Yuan

Department of Physics, Tsinghua University, Beijing, China
M. Ahmad, Z. Hu, Y. Wang

Institute of High Energy Physics, Beijing, China
E. Chapon, G.M. Chen[9], H.S. Chen[9], M. Chen, C.H. Jiang, D. Leggat, H. Liao, Z. Liu, A. Spiezia, J. Tao, J. Wang, H. Zhang, S. Zhang[9], J. Zhao

State Key Laboratory of Nuclear Physics and Technology, Peking University, Beijing, China
A. Agapitos, Y. Ban, C. Chen, G. Chen, A. Levin, J. Li, L. Li, Q. Li, X. Lyu, Y. Mao, S.J. Qian, D. Wang, Q. Wang, J. Xiao

Sun Yat-Sen University, Guangzhou, China
Z. You

Zhejiang University, Hangzhou, China
M. Xiao

Universidad de Los Andes, Bogota, Colombia
C. Avila, A. Cabrera, C. Florez, J. Fraga, A. Sarkar, M.A. Segura Delgado

Universidad de Antioquia, Medellin, Colombia
J. Mejia Guisao, F. Ramirez, J.D. Ruiz Alvarez, C.A. Salazar González, N. Vanegas Arbelaez

University of Split, Faculty of Electrical Engineering, Mechanical Engineering and Naval Architecture, Split, Croatia
D. Giljanovic, N. Godinovic, D. Lelas, I. Puljak, T. Sculac

University of Split, Faculty of Science, Split, Croatia
Z. Antunovic, M. Kovac

Institute Rudjer Boskovic, Zagreb, Croatia
V. Brigljevic, D. Ferencek, D. Majumder, B. Mesic, M. Roguljic, A. Starodumov[10], T. Susa

JHEP08(2020)139

University of Cyprus, Nicosia, Cyprus

M.W. Ather, A. Attikis, E. Erodotou, A. Ioannou, G. Kole, M. Kolosova, S. Konstantinou, G. Mavromanolakis, J. Mousa, C. Nicolaou, F. Ptochos, P.A. Razis, H. Rykaczewski, H. Saka, D. Tsiakkouri

Charles University, Prague, Czech Republic

M. Finger[11], M. Finger Jr.[11], A. Kveton, J. Tomsa

Escuela Politecnica Nacional, Quito, Ecuador

E. Ayala

Universidad San Francisco de Quito, Quito, Ecuador

E. Carrera Jarrin

Academy of Scientific Research and Technology of the Arab Republic of Egypt, Egyptian Network of High Energy Physics, Cairo, Egypt

E. Salama[12,13]

Center for High Energy Physics (CHEP-FU), Fayoum University, El-Fayoum, Egypt

A. Lotfy, M.A. Mahmoud

National Institute of Chemical Physics and Biophysics, Tallinn, Estonia

S. Bhowmik, A. Carvalho Antunes De Oliveira, R.K. Dewanjee, K. Ehataht, M. Kadastik, M. Raidal, C. Veelken

Department of Physics, University of Helsinki, Helsinki, Finland

P. Eerola, L. Forthomme, H. Kirschenmann, K. Osterberg, M. Voutilainen

Helsinki Institute of Physics, Helsinki, Finland

E. Brücken, F. Garcia, J. Havukainen, V. Karimäki, M.S. Kim, R. Kinnunen, T. Lampén, K. Lassila-Perini, S. Laurila, S. Lehti, T. Lindén, H. Siikonen, E. Tuominen, J. Tuominiemi

Lappeenranta University of Technology, Lappeenranta, Finland

P. Luukka, T. Tuuva

IRFU, CEA, Université Paris-Saclay, Gif-sur-Yvette, France

M. Besancon, F. Couderc, M. Dejardin, D. Denegri, J.L. Faure, F. Ferri, S. Ganjour, A. Givernaud, P. Gras, G. Hamel de Monchenault, P. Jarry, C. Leloup, B. Lenzi, E. Locci, J. Malcles, J. Rander, A. Rosowsky, M.Ö. Sahin, A. Savoy-Navarro[14], M. Titov, G.B. Yu

Laboratoire Leprince-Ringuet, CNRS/IN2P3, Ecole Polytechnique, Institut Polytechnique de Paris, France

S. Ahuja, C. Amendola, F. Beaudette, M. Bonanomi, P. Busson, C. Charlot, O. Davignon, B. Diab, G. Falmagne, R. Granier de Cassagnac, I. Kucher, A. Lobanov, C. Martin Perez, M. Nguyen, C. Ochando, P. Paganini, J. Rembser, R. Salerno, J.B. Sauvan, Y. Sirois, A. Zabi, A. Zghiche

JHEP08(2020)139

Université de Strasbourg, CNRS, IPHC UMR 7178, Strasbourg, France

J.-L. Agram[15], J. Andrea, D. Bloch, G. Bourgatte, J.-M. Brom, E.C. Chabert, C. Collard, J.-C. Fontaine[15], D. Gelé, U. Goerlach, C. Grimault, A.-C. Le Bihan, P. Van Hove

Université de Lyon, Université Claude Bernard Lyon 1, CNRS-IN2P3, Institut de Physique Nucléaire de Lyon, Villeurbanne, France

E. Asilar, S. Beauceron, C. Bernet, G. Boudoul, C. Camen, A. Carle, N. Chanon, R. Chierici, D. Contardo, P. Depasse, H. El Mamouni, J. Fay, S. Gascon, M. Gouzevitch, B. Ille, Sa. Jain, I.B. Laktineh, H. Lattaud, A. Lesauvage, M. Lethuillier, L. Mirabito, L. Torterotot, G. Touquet, M. Vander Donckt, S. Viret

Georgian Technical University, Tbilisi, Georgia

A. Khvedelidze[11]

Tbilisi State University, Tbilisi, Georgia

Z. Tsamalaidze[11]

RWTH Aachen University, I. Physikalisches Institut, Aachen, Germany

L. Feld, K. Klein, M. Lipinski, D. Meuser, A. Pauls, M. Preuten, M.P. Rauch, J. Schulz, M. Teroerde

RWTH Aachen University, III. Physikalisches Institut A, Aachen, Germany

D. Eliseev, M. Erdmann, P. Fackeldey, B. Fischer, S. Ghosh, T. Hebbeker, K. Hoepfner, H. Keller, L. Mastrolorenzo, M. Merschmeyer, A. Meyer, P. Millet, G. Mocellin, S. Mondal, S. Mukherjee, D. Noll, A. Novak, T. Pook, A. Pozdnyakov, T. Quast, M. Radziej, Y. Rath, H. Reithler, J. Roemer, A. Schmidt, S.C. Schuler, A. Sharma, S. Wiedenbeck, S. Zaleski

RWTH Aachen University, III. Physikalisches Institut B, Aachen, Germany

C. Dziwok, G. Flügge, W. Haj Ahmad[16], O. Hlushchenko, T. Kress, A. Nowack, C. Pistone, O. Pooth, D. Roy, H. Sert, A. Stahl[17], T. Ziemons

Deutsches Elektronen-Synchrotron, Hamburg, Germany

H. Aarup Petersen, M. Aldaya Martin, P. Asmuss, I. Babounikau, S. Baxter, O. Behnke, A. Bermúdez Martínez, A.A. Bin Anuar, K. Borras[18], V. Botta, D. Brunner, A. Campbell, A. Cardini, P. Connor, S. Consuegra Rodríguez, V. Danilov, A. De Wit, M.M. Defranchis, L. Didukh, D. Domínguez Damiani, G. Eckerlin, D. Eckstein, T. Eichhorn, A. Elwood, L.I. Estevez Banos, E. Gallo[19], A. Geiser, A. Giraldi, A. Grohsjean, M. Guthoff, M. Haranko, A. Harb, A. Jafari[20], N.Z. Jomhari, H. Jung, A. Kasem[18], M. Kasemann, H. Kaveh, J. Keaveney, C. Kleinwort, J. Knolle, D. Krücker, W. Lange, T. Lenz, J. Lidrych, K. Lipka, W. Lohmann[21], R. Mankel, I.-A. Melzer-Pellmann, J. Metwally, A.B. Meyer, M. Meyer, M. Missiroli, J. Mnich, A. Mussgiller, V. Myronenko, Y. Otarid, D. Pérez Adán, S.K. Pflitsch, D. Pitzl, A. Raspereza, A. Saibel, M. Savitskyi, V. Scheurer, P. Schütze, C. Schwanenberger, R. Shevchenko, A. Singh, R.E. Sosa Ricardo, H. Tholen, N. Tonon, O. Turkot, A. Vagnerini, M. Van De Klundert, R. Walsh, D. Walter, Y. Wen, K. Wichmann, C. Wissing, S. Wuchterl, O. Zenaiev, R. Zlebcik

JHEP08(2020)139

University of Hamburg, Hamburg, Germany

R. Aggleton, S. Bein, L. Benato, A. Benecke, K. De Leo, T. Dreyer, A. Ebrahimi, F. Feindt, A. Fröhlich, C. Garbers, E. Garutti, D. Gonzalez, P. Gunnellini, J. Haller, A. Hinzmann, A. Karavdina, G. Kasieczka, R. Klanner, R. Kogler, S. Kurz, V. Kutzner, J. Lange, T. Lange, A. Malara, J. Multhaup, C.E.N. Niemeyer, A. Nigamova, K.J. Pena Rodriguez, A. Reimers, O. Rieger, P. Schleper, S. Schumann, J. Schwandt, D. Schwarz, J. Sonneveld, H. Stadie, G. Steinbrück, B. Vormwald, I. Zoi

Karlsruher Institut fuer Technologie, Karlsruhe, Germany

M. Akbiyik, M. Baselga, S. Baur, J. Bechtel, T. Berger, E. Butz, R. Caspart, T. Chwalek, W. De Boer, A. Dierlamm, K. El Morabit, N. Faltermann, K. Flöh, M. Giffels, A. Gottmann, F. Hartmann[17], C. Heidecker, U. Husemann, M.A. Iqbal, I. Katkov[22], S. Kudella, S. Maier, M. Metzler, S. Mitra, M.U. Mozer, D. Müller, Th. Müller, M. Musich, G. Quast, K. Rabbertz, J. Rauser, D. Savoiu, D. Schäfer, M. Schnepf, M. Schröder, D. Seith, I. Shvetsov, H.J. Simonis, R. Ulrich, M. Wassmer, M. Weber, C. Wöhrmann, R. Wolf, S. Wozniewski

Institute of Nuclear and Particle Physics (INPP), NCSR Demokritos, Aghia Paraskevi, Greece

G. Anagnostou, P. Asenov, G. Daskalakis, T. Geralis, A. Kyriakis, D. Loukas, G. Paspalaki, A. Stakia

National and Kapodistrian University of Athens, Athens, Greece

M. Diamantopoulou, D. Karasavvas, G. Karathanasis, P. Kontaxakis, C.K. Koraka, A. Manousakis-katsikakis, A. Panagiotou, I. Papavergou, N. Saoulidou, K. Theofilatos, K. Vellidis, E. Vourliotis

National Technical University of Athens, Athens, Greece

G. Bakas, K. Kousouris, I. Papakrivopoulos, G. Tsipolitis, A. Zacharopoulou

University of Ioánnina, Ioánnina, Greece

I. Evangelou, C. Foudas, P. Gianneios, P. Katsoulis, P. Kokkas, S. Mallios, K. Manitara, N. Manthos, I. Papadopoulos, J. Strologas, D. Tsitsonis

MTA-ELTE Lendület CMS Particle and Nuclear Physics Group, Eötvös Loránd University, Budapest, Hungary

M. Bartók[23], R. Chudasama, M. Csanad, M.M.A. Gadallah[24], P. Major, K. Mandal, A. Mehta, G. Pasztor, O. Surányi, G.I. Veres

Wigner Research Centre for Physics, Budapest, Hungary

G. Bencze, C. Hajdu, D. Horvath[25], F. Sikler, V. Veszpremi, G. Vesztergombi[†]

Institute of Nuclear Research ATOMKI, Debrecen, Hungary

N. Beni, S. Czellar, J. Karancsi[23], J. Molnar, Z. Szillasi, D. Teyssier

Institute of Physics, University of Debrecen, Debrecen, Hungary

P. Raics, Z.L. Trocsanyi, B. Ujvari

JHEP08(2020)139

Eszterhazy Karoly University, Karoly Robert Campus, Gyongyos, Hungary
T. Csorgo, S. Lökös[26], F. Nemes, T. Novak

Indian Institute of Science (IISc), Bangalore, India
S. Choudhury, J.R. Komaragiri, D. Kumar, L. Panwar, P.C. Tiwari

National Institute of Science Education and Research, HBNI, Bhubaneswar, India
S. Bahinipati[27], D. Dash, C. Kar, P. Mal, T. Mishra, V.K. Muraleedharan Nair Bindhu, A. Nayak[28], D.K. Sahoo[27], N. Sur, S.K. Swain

Panjab University, Chandigarh, India
S. Bansal, S.B. Beri, V. Bhatnagar, S. Chauhan, N. Dhingra[29], R. Gupta, A. Kaur, A. Kaur, S. Kaur, P. Kumari, M. Lohan, M. Meena, K. Sandeep, S. Sharma, J.B. Singh, A.K. Virdi

University of Delhi, Delhi, India
A. Ahmed, A. Bhardwaj, B.C. Choudhary, R.B. Garg, M. Gola, S. Keshri, A. Kumar, M. Naimuddin, P. Priyanka, K. Ranjan, A. Shah, R. Sharma

Saha Institute of Nuclear Physics, HBNI, Kolkata, India
M. Bharti[30], R. Bhattacharya, S. Bhattacharya, D. Bhowmik, S. Dutta, S. Ghosh, B. Gomber[31], M. Maity[32], K. Mondal, S. Nandan, P. Palit, A. Purohit, P.K. Rout, G. Saha, S. Sarkar, M. Sharan, B. Singh[30], S. Thakur[30]

Indian Institute of Technology Madras, Madras, India
P.K. Behera, S.C. Behera, P. Kalbhor, A. Muhammad, R. Pradhan, P.R. Pujahari, A. Sharma, A.K. Sikdar

Bhabha Atomic Research Centre, Mumbai, India
D. Dutta, V. Jha, D.K. Mishra, K. Naskar[33], P.K. Netrakanti, L.M. Pant, P. Shukla

Tata Institute of Fundamental Research-A, Mumbai, India
T. Aziz, M.A. Bhat, S. Dugad, R. Kumar Verma, U. Sarkar

Tata Institute of Fundamental Research-B, Mumbai, India
S. Banerjee, S. Bhattacharya, S. Chatterjee, P. Das, M. Guchait, S. Karmakar, S. Kumar, G. Majumder, K. Mazumdar, S. Mukherjee, D. Roy, N. Sahoo

Indian Institute of Science Education and Research (IISER), Pune, India
S. Dube, B. Kansal, A. Kapoor, K. Kothekar, S. Pandey, A. Rane, A. Rastogi, S. Sharma

Isfahan University of Technology, Isfahan, Iran
H. Bakhshiansohi[34]

Institute for Research in Fundamental Sciences (IPM), Tehran, Iran
S. Chenarani[35], S.M. Etesami, M. Khakzad, M. Mohammadi Najafabadi, M. Naseri

University College Dublin, Dublin, Ireland
M. Felcini, M. Grunewald

JHEP08(2020)139

INFN Sezione di Bari[a], Università di Bari[b], Politecnico di Bari[c], Bari, Italy
M. Abbrescia[a,b], R. Aly[a,b,36], C. Calabria[a,b], A. Colaleo[a], D. Creanza[a,c], N. De Filippis[a,c], M. De Palma[a,b], A. Di Florio[a,b], A. Di Pilato[a,b], W. Elmetenawee[a,b], L. Fiore[a], A. Gelmi[a,b], G. Iaselli[a,c], M. Ince[a,b], S. Lezki[a,b], G. Maggi[a,c], M. Maggi[a], I. Margjeka[a,b], J.A. Merlin[a], S. My[a,b], S. Nuzzo[a,b], A. Pompili[a,b], G. Pugliese[a,c], A. Ranieri[a], G. Selvaggi[a,b], L. Silvestris[a], F.M. Simone[a,b], R. Venditti[a], P. Verwilligen[a]

INFN Sezione di Bologna[a], Università di Bologna[b], Bologna, Italy
G. Abbiendi[a], C. Battilana[a,b], D. Bonacorsi[a,b], L. Borgonovi[a,b], S. Braibant-Giacomelli[a,b], R. Campanini[a,b], P. Capiluppi[a,b], A. Castro[a,b], F.R. Cavallo[a], C. Ciocca[a], M. Cuffiani[a,b], G.M. Dallavalle[a], T. Diotalevi[a,b], F. Fabbri[a], A. Fanfani[a,b], E. Fontanesi[a,b], P. Giacomelli[a], C. Grandi[a], L. Guiducci[a,b], F. Iemmi[a,b], S. Lo Meo[a,37], S. Marcellini[a], G. Masetti[a], F.L. Navarria[a,b], A. Perrotta[a], F. Primavera[a,b], A.M. Rossi[a,b], T. Rovelli[a,b], G.P. Siroli[a,b], N. Tosi[a]

INFN Sezione di Catania[a], Università di Catania[b], Catania, Italy
S. Albergo[a,b,38], S. Costa[a,b], A. Di Mattia[a], R. Potenza[a,b], A. Tricomi[a,b,38], C. Tuve[a,b]

INFN Sezione di Firenze[a], Università di Firenze[b], Firenze, Italy
G. Barbagli[a], A. Cassese[a], R. Ceccarelli[a,b], V. Ciulli[a,b], C. Civinini[a], R. D'Alessandro[a,b], F. Fiori[a,c], E. Focardi[a,b], G. Latino[a,b], P. Lenzi[a,b], M. Lizzo[a,b], M. Meschini[a], S. Paoletti[a], R. Seidita[a,b], G. Sguazzoni[a], L. Viliani[a]

INFN Laboratori Nazionali di Frascati, Frascati, Italy
L. Benussi, S. Bianco, D. Piccolo

INFN Sezione di Genova[a], Università di Genova[b], Genova, Italy
M. Bozzo[a,b], F. Ferro[a], R. Mulargia[a,b], E. Robutti[a], S. Tosi[a,b]

INFN Sezione di Milano-Bicocca[a], Università di Milano-Bicocca[b], Milano, Italy
A. Benaglia[a], A. Beschi[a,b], F. Brivio[a,b], F. Cetorelli[a,b], V. Ciriolo[a,b,17], F. De Guio[a,b], M.E. Dinardo[a,b], P. Dini[a], S. Gennai[a], A. Ghezzi[a,b], P. Govoni[a,b], L. Guzzi[a,b], M. Malberti[a], S. Malvezzi[a], D. Menasce[a], F. Monti[a,b], L. Moroni[a], M. Paganoni[a,b], D. Pedrini[a], S. Ragazzi[a,b], T. Tabarelli de Fatis[a,b], D. Valsecchi[a,b,17], D. Zuolo[a,b]

INFN Sezione di Napoli[a], Università di Napoli 'Federico II'[b], Napoli, Italy, Università della Basilicata[c], Potenza, Italy, Università G. Marconi[d], Roma, Italy
S. Buontempo[a], N. Cavallo[a,c], A. De Iorio[a,b], F. Fabozzi[a,c], F. Fienga[a], A.O.M. Iorio[a,b], L. Layer[a,b], L. Lista[a,b], S. Meola[a,d,17], P. Paolucci[a,17], B. Rossi[a], C. Sciacca[a,b], E. Voevodina[a,b]

INFN Sezione di Padova[a], Università di Padova[b], Padova, Italy, Università di Trento[c], Trento, Italy
P. Azzi[a], N. Bacchetta[a], D. Bisello[a,b], A. Boletti[a,b], A. Bragagnolo[a,b], R. Carlin[a,b], P. Checchia[a], P. De Castro Manzano[a], T. Dorigo[a], U. Dosselli[a], F. Gasparini[a,b], U. Gasparini[a,b], S.Y. Hoh[a,b], M. Margoni[a,b], A.T. Meneguzzo[a,b], M. Presilla[b],

JHEP08(2020)139

P. Ronchese[a,b], R. Rossin[a,b], G. Strong, A. Tiko[a], M. Tosi[a,b], H. YARAR[a,b], M. Zanetti[a,b], P. Zotto[a,b], A. Zucchetta[a,b], G. Zumerle[a,b]

INFN Sezione di Pavia[a], Università di Pavia[b], Pavia, Italy

A. Braghieri[a], S. Calzaferri[a,b], D. Fiorina[a,b], P. Montagna[a,b], S.P. Ratti[a,b], V. Re[a], M. Ressegotti[a,b], C. Riccardi[a,b], P. Salvini[a], I. Vai[a], P. Vitulo[a,b]

INFN Sezione di Perugia[a], Università di Perugia[b], Perugia, Italy

M. Biasini[a,b], G.M. Bilei[a], D. Ciangottini[a,b], L. Fanò[a,b], P. Lariccia[a,b], G. Mantovani[a,b], V. Mariani[a,b], M. Menichelli[a], F. Moscatelli[a], A. Rossi[a,b], A. Santocchia[a,b], D. Spiga[a], T. Tedeschi[a,b]

INFN Sezione di Pisa[a], Università di Pisa[b], Scuola Normale Superiore di Pisa[c], Pisa, Italy

K. Androsov[a], P. Azzurri[a], G. Bagliesi[a], V. Bertacchi[a,c], L. Bianchini[a], T. Boccali[a], R. Castaldi[a], M.A. Ciocci[a,b], R. Dell'Orso[a], M.R. Di Domenico, S. Donato[a], L. Giannini[a,c], A. Giassi[a], M.T. Grippo[a], F. Ligabue[a,c], E. Manca[a,c], G. Mandorli[a,c], A. Messineo[a,b], F. Palla[a], A. Rizzi[a,b], G. Rolandi[a,c], S. Roy Chowdhury[a,c], A. Scribano[a], N. Shafiei, P. Spagnolo[a], R. Tenchini[a], G. Tonelli[a,b], N. Turini[a], A. Venturi[a], P.G. Verdini[a]

INFN Sezione di Roma[a], Sapienza Università di Roma[b], Rome, Italy

F. Cavallari[a], M. Cipriani[a,b], D. Del Re[a,b], E. Di Marco[a], M. Diemoz[a], E. Longo[a,b], P. Meridiani[a], G. Organtini[a,b], F. Pandolfi[a], R. Paramatti[a,b], C. Quaranta[a,b], S. Rahatlou[a,b], C. Rovelli[a], F. Santanastasio[a,b], L. Soffi[a,b], R. Tramontano[a,b]

INFN Sezione di Torino[a], Università di Torino[b], Torino, Italy, Università del Piemonte Orientale[c], Novara, Italy

N. Amapane[a,b], R. Arcidiacono[a,c], S. Argiro[a,b], M. Arneodo[a,c], N. Bartosik[a], R. Bellan[a,b], A. Bellora[a,b], C. Biino[a], A. Cappati[a,b], N. Cartiglia[a], S. Cometti[a], M. Costa[a,b], R. Covarelli[a,b], N. Demaria[a], B. Kiani[a,b], F. Legger[a], C. Mariotti[a], S. Maselli[a], E. Migliore[a,b], V. Monaco[a,b], E. Monteil[a,b], M. Monteno[a], M.M. Obertino[a,b], G. Ortona[a], L. Pacher[a,b], N. Pastrone[a], M. Pelliccioni[a], G.L. Pinna Angioni[a,b], M. Ruspa[a,c], R. Salvatico[a,b], F. Siviero[a,b], V. Sola[a], A. Solano[a,b], D. Soldi[a,b], A. Staiano[a], D. Trocino[a,b]

INFN Sezione di Trieste[a], Università di Trieste[b], Trieste, Italy

S. Belforte[a], V. Candelise[a,b], M. Casarsa[a], F. Cossutti[a], A. Da Rold[a,b], G. Della Ricca[a,b], F. Vazzoler[a,b]

Kyungpook National University, Daegu, Korea

S. Dogra, C. Huh, B. Kim, D.H. Kim, G.N. Kim, J. Lee, S.W. Lee, C.S. Moon, Y.D. Oh, S.I. Pak, S. Sekmen, Y.C. Yang

Chonnam National University, Institute for Universe and Elementary Particles, Kwangju, Korea

H. Kim, D.H. Moon

Hanyang University, Seoul, Korea

B. Francois, T.J. Kim, J. Park

JHEP08(2020)139

Korea University, Seoul, Korea
S. Cho, S. Choi, Y. Go, S. Ha, B. Hong, K. Lee, K.S. Lee, J. Lim, J. Park, S.K. Park, Y. Roh, J. Yoo

Kyung Hee University, Department of Physics, Seoul, Republic of Korea
J. Goh, A. Gurtu

Sejong University, Seoul, Korea
H.S. Kim, Y. Kim

Seoul National University, Seoul, Korea
J. Almond, J.H. Bhyun, J. Choi, S. Jeon, J. Kim, J.S. Kim, S. Ko, H. Kwon, H. Lee, K. Lee, S. Lee, K. Nam, B.H. Oh, M. Oh, S.B. Oh, B.C. Radburn-Smith, H. Seo, U.K. Yang, I. Yoon

University of Seoul, Seoul, Korea
D. Jeon, J.H. Kim, B. Ko, J.S.H. Lee, I.C. Park, I.J. Watson

Yonsei University, Department of Physics, Seoul, Korea
H.D. Yoo

Sungkyunkwan University, Suwon, Korea
Y. Choi, C. Hwang, Y. Jeong, H. Lee, J. Lee, Y. Lee, I. Yu

Riga Technical University, Riga, Latvia
V. Veckalns[39]

Vilnius University, Vilnius, Lithuania
A. Juodagalvis, A. Rinkevicius, G. Tamulaitis

National Centre for Particle Physics, Universiti Malaya, Kuala Lumpur, Malaysia
W.A.T. Wan Abdullah, M.N. Yusli, Z. Zolkapli

Universidad de Sonora (UNISON), Hermosillo, Mexico
J.F. Benitez, A. Castaneda Hernandez, J.A. Murillo Quijada, L. Valencia Palomo

Centro de Investigacion y de Estudios Avanzados del IPN, Mexico City, Mexico
H. Castilla-Valdez, E. De La Cruz-Burelo, I. Heredia-De La Cruz[40], R. Lopez-Fernandez, A. Sanchez-Hernandez

Universidad Iberoamericana, Mexico City, Mexico
S. Carrillo Moreno, C. Oropeza Barrera, M. Ramirez-Garcia, F. Vazquez Valencia

Benemerita Universidad Autonoma de Puebla, Puebla, Mexico
J. Eysermans, I. Pedraza, H.A. Salazar Ibarguen, C. Uribe Estrada

Universidad Autónoma de San Luis Potosí, San Luis Potosí, Mexico
A. Morelos Pineda

University of Montenegro, Podgorica, Montenegro
J. Mijuskovic[4], N. Raicevic

JHEP08(2020)139

University of Auckland, Auckland, New Zealand
D. Krofcheck

University of Canterbury, Christchurch, New Zealand
S. Bheesette, P.H. Butler

National Centre for Physics, Quaid-I-Azam University, Islamabad, Pakistan
A. Ahmad, M. Ahmad, M.I. Asghar, M.I.M. Awan, Q. Hassan, H.R. Hoorani, W.A. Khan, M.A. Shah, M. Shoaib, M. Waqas

AGH University of Science and Technology Faculty of Computer Science, Electronics and Telecommunications, Krakow, Poland
V. Avati, L. Grzanka, M. Malawski

National Centre for Nuclear Research, Swierk, Poland
H. Bialkowska, M. Bluj, B. Boimska, T. Frueboes, M. Górski, M. Kazana, M. Szleper, P. Traczyk, P. Zalewski

Institute of Experimental Physics, Faculty of Physics, University of Warsaw, Warsaw, Poland
K. Bunkowski, A. Byszuk[41], K. Doroba, A. Kalinowski, M. Konecki, J. Krolikowski, M. Olszewski, M. Walczak

Laboratório de Instrumentação e Física Experimental de Partículas, Lisboa, Portugal
M. Araujo, P. Bargassa, D. Bastos, A. Di Francesco, P. Faccioli, B. Galinhas, M. Gallinaro, J. Hollar, N. Leonardo, T. Niknejad, J. Seixas, K. Shchelina, O. Toldaiev, J. Varela

Joint Institute for Nuclear Research, Dubna, Russia
V. Alexakhin, A. Baginyan, P. Bunin, I. Golutvin, I. Gorbunov, V. Karjavine, I. Kashunin, V. Korenkov, A. Lanev, A. Malakhov, V. Matveev[42,43], P. Moisenz, V. Palichik, V. Perelygin, M. Savina, D. Seitova, S. Shmatov, O. Teryaev, B.S. Yuldashev[44], A. Zarubin, V. Zhiltsov

Petersburg Nuclear Physics Institute, Gatchina (St. Petersburg), Russia
G. Gavrilov, V. Golovtcov, Y. Ivanov, V. Kim[45], E. Kuznetsova[46], V. Murzin, V. Oreshkin, I. Smirnov, D. Sosnov, V. Sulimov, L. Uvarov, S. Volkov, A. Vorobyev

Institute for Nuclear Research, Moscow, Russia
Yu. Andreev, A. Dermenev, S. Gninenko, N. Golubev, A. Karneyeu, M. Kirsanov, N. Krasnikov, A. Pashenkov, G. Pivovarov, D. Tlisov, A. Toropin

Institute for Theoretical and Experimental Physics named by A.I. Alikhanov of NRC 'Kurchatov Institute', Moscow, Russia
V. Epshteyn, V. Gavrilov, N. Lychkovskaya, A. Nikitenko[47], V. Popov, I. Pozdnyakov, G. Safronov, A. Spiridonov, A. Stepennov, M. Toms, E. Vlasov, A. Zhokin

Moscow Institute of Physics and Technology, Moscow, Russia
T. Aushev

JHEP08(2020)139

National Research Nuclear University 'Moscow Engineering Physics Institute' (MEPhI), Moscow, Russia

M. Chadeeva[48], A. Oskin, P. Parygin, S. Polikarpov[48], E. Zhemchugov

P.N. Lebedev Physical Institute, Moscow, Russia

V. Andreev, M. Azarkin, I. Dremin, M. Kirakosyan, A. Terkulov

Skobeltsyn Institute of Nuclear Physics, Lomonosov Moscow State University, Moscow, Russia

A. Baskakov, A. Belyaev, E. Boos, V. Bunichev, M. Dubinin[49], L. Dudko, V. Klyukhin, O. Kodolova, I. Lokhtin, S. Obraztsov, M. Perfilov, S. Petrushanko, V. Savrin

Novosibirsk State University (NSU), Novosibirsk, Russia

V. Blinov[50], T. Dimova[50], L. Kardapoltsev[50], I. Ovtin[50], Y. Skovpen[50]

Institute for High Energy Physics of National Research Centre 'Kurchatov Institute', Protvino, Russia

I. Azhgirey, I. Bayshev, V. Kachanov, A. Kalinin, D. Konstantinov, V. Petrov, R. Ryutin, A. Sobol, S. Troshin, N. Tyurin, A. Uzunian, A. Volkov

National Research Tomsk Polytechnic University, Tomsk, Russia

A. Babaev, A. Iuzhakov, V. Okhotnikov

Tomsk State University, Tomsk, Russia

V. Borchsh, V. Ivanchenko, E. Tcherniaev

University of Belgrade: Faculty of Physics and VINCA Institute of Nuclear Sciences, Serbia

P. Adzic[51], P. Cirkovic, M. Dordevic, P. Milenovic, J. Milosevic, M. Stojanovic

Centro de Investigaciones Energéticas Medioambientales y Tecnológicas (CIEMAT), Madrid, Spain

M. Aguilar-Benitez, J. Alcaraz Maestre, A. Álvarez Fernández, I. Bachiller, M. Barrio Luna, CristinaF. Bedoya, J.A. Brochero Cifuentes, C.A. Carrillo Montoya, M. Cepeda, M. Cerrada, N. Colino, B. De La Cruz, A. Delgado Peris, J.P. Fernández Ramos, J. Flix, M.C. Fouz, O. Gonzalez Lopez, S. Goy Lopez, J.M. Hernandez, M.I. Josa, D. Moran, Á. Navarro Tobar, A. Pérez-Calero Yzquierdo, J. Puerta Pelayo, I. Redondo, L. Romero, S. Sánchez Navas, M.S. Soares, A. Triossi, C. Willmott

Universidad Autónoma de Madrid, Madrid, Spain

C. Albajar, J.F. de Trocóniz, R. Reyes-Almanza

Universidad de Oviedo, Instituto Universitario de Ciencias y Tecnologías Espaciales de Asturias (ICTEA), Oviedo, Spain

B. Alvarez Gonzalez, J. Cuevas, C. Erice, J. Fernandez Menendez, S. Folgueras, I. Gonzalez Caballero, E. Palencia Cortezon, C. Ramón Álvarez, V. Rodríguez Bouza, S. Sanchez Cruz

JHEP08(2020)139

Instituto de Física de Cantabria (IFCA), CSIC-Universidad de Cantabria, Santander, Spain

I.J. Cabrillo, A. Calderon, B. Chazin Quero, J. Duarte Campderros, M. Fernandez, P.J. Fernández Manteca, A. García Alonso, G. Gomez, C. Martinez Rivero, P. Martinez Ruiz del Arbol, F. Matorras, J. Piedra Gomez, C. Prieels, F. Ricci-Tam, T. Rodrigo, A. Ruiz-Jimeno, L. Russo[52], L. Scodellaro, I. Vila, J.M. Vizan Garcia

University of Colombo, Colombo, Sri Lanka

MK Jayananda, B. Kailasapathy[53], D.U.J. Sonnadara, DDC Wickramarathna

University of Ruhuna, Department of Physics, Matara, Sri Lanka

W.G.D. Dharmaratna, K. Liyanage, N. Perera, N. Wickramage

CERN, European Organization for Nuclear Research, Geneva, Switzerland

T.K. Aarrestad, D. Abbaneo, B. Akgun, E. Auffray, G. Auzinger, J. Baechler, P. Baillon, A.H. Ball, D. Barney, J. Bendavid, M. Bianco, A. Bocci, P. Bortignon, E. Bossini, E. Brondolin, T. Camporesi, G. Cerminara, L. Cristella, D. d'Enterria, A. Dabrowski, N. Daci, V. Daponte, A. David, A. De Roeck, M. Deile, R. Di Maria, M. Dobson, M. Dünser, N. Dupont, A. Elliott-Peisert, N. Emriskova, F. Fallavollita[54], D. Fasanella, S. Fiorendi, G. Franzoni, J. Fulcher, W. Funk, S. Giani, D. Gigi, K. Gill, F. Glege, L. Gouskos, M. Gruchala, M. Guilbaud, D. Gulhan, J. Hegeman, Y. Iiyama, V. Innocente, T. James, P. Janot, J. Kaspar, J. Kieseler, M. Komm, N. Kratochwil, C. Lange, P. Lecoq, K. Long, C. Lourenço, L. Malgeri, M. Mannelli, A. Massironi, F. Meijers, S. Mersi, E. Meschi, F. Moortgat, M. Mulders, J. Ngadiuba, J. Niedziela, S. Orfanelli, L. Orsini, F. Pantaleo[17], L. Pape, E. Perez, M. Peruzzi, A. Petrilli, G. Petrucciani, A. Pfeiffer, M. Pierini, F.M. Pitters, D. Rabady, A. Racz, M. Rieger, M. Rovere, H. Sakulin, J. Salfeld-Nebgen, S. Scarfi, C. Schäfer, C. Schwick, M. Selvaggi, A. Sharma, P. Silva, W. Snoeys, P. Sphicas[55], J. Steggemann, S. Summers, V.R. Tavolaro, D. Treille, A. Tsirou, G.P. Van Onsem, A. Vartak, M. Verzetti, K.A. Wozniak, W.D. Zeuner

Paul Scherrer Institut, Villigen, Switzerland

L. Caminada[56], W. Erdmann, R. Horisberger, Q. Ingram, H.C. Kaestli, D. Kotlinski, U. Langenegger, T. Rohe

ETH Zurich — Institute for Particle Physics and Astrophysics (IPA), Zurich, Switzerland

M. Backhaus, P. Berger, A. Calandri, N. Chernyavskaya, G. Dissertori, M. Dittmar, M. Donegà, C. Dorfer, T. Gadek, T.A. Gómez Espinosa, C. Grab, D. Hits, W. Lustermann, A.-M. Lyon, R.A. Manzoni, M.T. Meinhard, F. Micheli, P. Musella, F. Nessi-Tedaldi, F. Pauss, V. Perovic, G. Perrin, L. Perrozzi, S. Pigazzini, M.G. Ratti, M. Reichmann, C. Reissel, T. Reitenspiess, B. Ristic, D. Ruini, D.A. Sanz Becerra, M. Schönenberger, L. Shchutska, V. Stampf, M.L. Vesterbacka Olsson, R. Wallny, D.H. Zhu

Universität Zürich, Zurich, Switzerland

C. Amsler[57], C. Botta, D. Brzhechko, M.F. Canelli, A. De Cosa, R. Del Burgo, J.K. Heikkilä, M. Huwiler, B. Kilminster, S. Leontsinis, A. Macchiolo, V.M. Mikuni, U. Molinatti, I. Neutelings, G. Rauco, P. Robmann, K. Schweiger, Y. Takahashi, S. Wertz

JHEP08(2020)139

National Central University, Chung-Li, Taiwan

C. Adloff[58], C.M. Kuo, W. Lin, A. Roy, T. Sarkar[32], S.S. Yu

National Taiwan University (NTU), Taipei, Taiwan

L. Ceard, P. Chang, Y. Chao, K.F. Chen, P.H. Chen, W.-S. Hou, Y.y. Li, R.-S. Lu, E. Paganis, A. Psallidas, A. Steen, E. Yazgan

Chulalongkorn University, Faculty of Science, Department of Physics, Bangkok, Thailand

B. Asavapibhop, C. Asawatangtrakuldee, N. Srimanobhas

Çukurova University, Physics Department, Science and Art Faculty, Adana, Turkey

F. Boran, S. Damarseckin[59], Z.S. Demiroglu, F. Dolek, C. Dozen[60], I. Dumanoglu[61], E. Eskut, G. Gokbulut, Y. Guler, E. Gurpinar Guler[62], I. Hos[63], C. Isik, E.E. Kangal[64], O. Kara, A. Kayis Topaksu, U. Kiminsu, G. Onengut, K. Ozdemir[65], A. Polatoz, A.E. Simsek, B. Tali[66], U.G. Tok, S. Turkcapar, I.S. Zorbakir, C. Zorbilmez

Middle East Technical University, Physics Department, Ankara, Turkey

B. Isildak[67], G. Karapinar[68], K. Ocalan[69], M. Yalvac[70]

Bogazici University, Istanbul, Turkey

I.O. Atakisi, E. Gülmez, M. Kaya[71], O. Kaya[72], Ö. Özçelik, S. Tekten[73], E.A. Yetkin[74]

Istanbul Technical University, Istanbul, Turkey

A. Cakir, K. Cankocak[61], Y. Komurcu, S. Sen[75]

Istanbul University, Istanbul, Turkey

F. Aydogmus Sen, S. Cerci[66], B. Kaynak, S. Ozkorucuklu, D. Sunar Cerci[66]

Institute for Scintillation Materials of National Academy of Science of Ukraine, Kharkov, Ukraine

B. Grynyov

National Scientific Center, Kharkov Institute of Physics and Technology, Kharkov, Ukraine

L. Levchuk

University of Bristol, Bristol, United Kingdom

E. Bhal, S. Bologna, J.J. Brooke, D. Burns[76], E. Clement, D. Cussans, H. Flacher, J. Goldstein, G.P. Heath, H.F. Heath, L. Kreczko, B. Krikler, S. Paramesvaran, T. Sakuma, S. Seif El Nasr-Storey, V.J. Smith, J. Taylor, A. Titterton

Rutherford Appleton Laboratory, Didcot, United Kingdom

K.W. Bell, A. Belyaev[77], C. Brew, R.M. Brown, D.J.A. Cockerill, K.V. Ellis, K. Harder, S. Harper, J. Linacre, K. Manolopoulos, D.M. Newbold, E. Olaiya, D. Petyt, T. Reis, T. Schuh, C.H. Shepherd-Themistocleous, A. Thea, I.R. Tomalin, T. Williams

JHEP08(2020)139

Imperial College, London, United Kingdom

R. Bainbridge, P. Bloch, S. Bonomally, J. Borg, S. Breeze, O. Buchmuller, A. Bundock, V. Cepaitis, G.S. Chahal[78], D. Colling, P. Dauncey, G. Davies, M. Della Negra, P. Everaerts, G. Fedi, G. Hall, G. Iles, J. Langford, L. Lyons, A.-M. Magnan, S. Malik, A. Martelli, V. Milosevic, A. Morton, J. Nash[79], V. Palladino, M. Pesaresi, D.M. Raymond, A. Richards, A. Rose, E. Scott, C. Seez, A. Shtipliyski, M. Stoye, A. Tapper, K. Uchida, T. Virdee[17], N. Wardle, S.N. Webb, D. Winterbottom, A.G. Zecchinelli, S.C. Zenz

Brunel University, Uxbridge, United Kingdom

J.E. Cole, P.R. Hobson, A. Khan, P. Kyberd, C.K. Mackay, I.D. Reid, L. Teodorescu, S. Zahid

Baylor University, Waco, U.S.A.

A. Brinkerhoff, K. Call, B. Caraway, J. Dittmann, K. Hatakeyama, C. Madrid, B. McMaster, N. Pastika, C. Smith

Catholic University of America, Washington, DC, U.S.A.

R. Bartek, A. Dominguez, R. Uniyal, A.M. Vargas Hernandez

The University of Alabama, Tuscaloosa, U.S.A.

A. Buccilli, O. Charaf, S.I. Cooper, S.V. Gleyzer, C. Henderson, P. Rumerio, C. West

Boston University, Boston, U.S.A.

A. Akpinar, A. Albert, D. Arcaro, C. Cosby, Z. Demiragli, D. Gastler, C. Richardson, J. Rohlf, K. Salyer, D. Sperka, D. Spitzbart, I. Suarez, S. Yuan, D. Zou

Brown University, Providence, U.S.A.

G. Benelli, B. Burkle, X. Coubez[18], D. Cutts, Y.t. Duh, M. Hadley, U. Heintz, J.M. Hogan[80], K.H.M. Kwok, E. Laird, G. Landsberg, K.T. Lau, J. Lee, M. Narain, S. Sagir[81], R. Syarif, E. Usai, W.Y. Wong, D. Yu, W. Zhang

University of California, Davis, Davis, U.S.A.

R. Band, C. Brainerd, R. Breedon, M. Calderon De La Barca Sanchez, M. Chertok, J. Conway, R. Conway, P.T. Cox, R. Erbacher, C. Flores, G. Funk, J. Gunion, G. Haza, F. Jensen, W. Ko[†], O. Kukral, R. Lander, M. Mulhearn, D. Pellett, J. Pilot, M. Shi, D. Taylor, K. Tos, M. Tripathi, Z. Wang, Y. Yao, F. Zhang

University of California, Los Angeles, U.S.A.

M. Bachtis, C. Bravo, R. Cousins, A. Dasgupta, A. Florent, D. Hamilton, J. Hauser, M. Ignatenko, T. Lam, N. Mccoll, W.A. Nash, S. Regnard, D. Saltzberg, C. Schnaible, B. Stone, V. Valuev

University of California, Riverside, Riverside, U.S.A.

K. Burt, Y. Chen, R. Clare, J.W. Gary, S.M.A. Ghiasi Shirazi, G. Hanson, G. Karapostoli, O.R. Long, N. Manganelli, M. Olmedo Negrete, M.I. Paneva, W. Si, S. Wimpenny, Y. Zhang

JHEP08(2020)139

University of California, San Diego, La Jolla, U.S.A.

J.G. Branson, P. Chang, S. Cittolin, S. Cooperstein, N. Deelen, M. Derdzinski, J. Duarte, R. Gerosa, D. Gilbert, B. Hashemi, D. Klein, V. Krutelyov, J. Letts, M. Masciovecchio, S. May, S. Padhi, M. Pieri, V. Sharma, M. Tadel, F. Würthwein, A. Yagil

University of California, Santa Barbara — Department of Physics, Santa Barbara, U.S.A.

N. Amin, R. Bhandari, C. Campagnari, M. Citron, A. Dorsett, V. Dutta, J. Incandela, B. Marsh, H. Mei, A. Ovcharova, H. Qu, M. Quinnan, J. Richman, U. Sarica, D. Stuart, S. Wang

California Institute of Technology, Pasadena, U.S.A.

D. Anderson, A. Bornheim, O. Cerri, I. Dutta, J.M. Lawhorn, N. Lu, J. Mao, H.B. Newman, T.Q. Nguyen, J. Pata, M. Spiropulu, J.R. Vlimant, S. Xie, Z. Zhang, R.Y. Zhu

Carnegie Mellon University, Pittsburgh, U.S.A.

J. Alison, M.B. Andrews, T. Ferguson, T. Mudholkar, M. Paulini, M. Sun, I. Vorobiev, M. Weinberg

University of Colorado Boulder, Boulder, U.S.A.

J.P. Cumalat, W.T. Ford, E. MacDonald, T. Mulholland, R. Patel, A. Perloff, K. Stenson, K.A. Ulmer, S.R. Wagner

Cornell University, Ithaca, U.S.A.

J. Alexander, Y. Cheng, J. Chu, D.J. Cranshaw, A. Datta, A. Frankenthal, K. Mcdermott, J. Monroy, J.R. Patterson, D. Quach, A. Ryd, W. Sun, S.M. Tan, Z. Tao, J. Thom, P. Wittich, M. Zientek

Fermi National Accelerator Laboratory, Batavia, U.S.A.

S. Abdullin, M. Albrow, M. Alyari, G. Apollinari, A. Apresyan, A. Apyan, S. Banerjee, L.A.T. Bauerdick, A. Beretvas, D. Berry, J. Berryhill, P.C. Bhat, K. Burkett, J.N. Butler, A. Canepa, G.B. Cerati, H.W.K. Cheung, F. Chlebana, M. Cremonesi, V.D. Elvira, J. Freeman, Z. Gecse, E. Gottschalk, L. Gray, D. Green, S. Grünendahl, O. Gutsche, R.M. Harris, S. Hasegawa, R. Heller, T.C. Herwig, J. Hirschauer, B. Jayatilaka, S. Jindariani, M. Johnson, U. Joshi, T. Klijnsma, B. Klima, M.J. Kortelainen, S. Lammel, J. Lewis, D. Lincoln, R. Lipton, M. Liu, T. Liu, J. Lykken, K. Maeshima, D. Mason, P. McBride, P. Merkel, S. Mrenna, S. Nahn, V. O'Dell, V. Papadimitriou, K. Pedro, C. Pena[49], O. Prokofyev, F. Ravera, A. Reinsvold Hall, L. Ristori, B. Schneider, E. Sexton-Kennedy, N. Smith, A. Soha, W.J. Spalding, L. Spiegel, S. Stoynev, J. Strait, L. Taylor, S. Tkaczyk, N.V. Tran, L. Uplegger, E.W. Vaandering, M. Wang, H.A. Weber, A. Woodard

University of Florida, Gainesville, U.S.A.

D. Acosta, P. Avery, D. Bourilkov, L. Cadamuro, V. Cherepanov, F. Errico, R.D. Field, D. Guerrero, B.M. Joshi, M. Kim, J. Konigsberg, A. Korytov, K.H. Lo, K. Matchev, N. Menendez, G. Mitselmakher, D. Rosenzweig, K. Shi, J. Wang, S. Wang, X. Zuo

Florida International University, Miami, U.S.A.

Y.R. Joshi

JHEP08(2020)139

Florida State University, Tallahassee, U.S.A.

T. Adams, A. Askew, D. Diaz, R. Habibullah, S. Hagopian, V. Hagopian, K.F. Johnson, R. Khurana, T. Kolberg, G. Martinez, H. Prosper, C. Schiber, R. Yohay, J. Zhang

Florida Institute of Technology, Melbourne, U.S.A.

M.M. Baarmand, S. Butalla, T. Elkafrawy[13], M. Hohlmann, D. Noonan, M. Rahmani, M. Saunders, F. Yumiceva

University of Illinois at Chicago (UIC), Chicago, U.S.A.

M.R. Adams, L. Apanasevich, H. Becerril Gonzalez, R. Cavanaugh, X. Chen, S. Dittmer, O. Evdokimov, C.E. Gerber, D.A. Hangal, D.J. Hofman, V. Kumar, C. Mills, G. Oh, T. Roy, M.B. Tonjes, N. Varelas, J. Viinikainen, H. Wang, X. Wang, Z. Wu

The University of Iowa, Iowa City, U.S.A.

M. Alhusseini, B. Bilki[62], K. Dilsiz[82], S. Durgut, R.P. Gandrajula, M. Haytmyradov, V. Khristenko, O.K. Köseyan, J.-P. Merlo, A. Mestvirishvili[83], A. Moeller, J. Nachtman, H. Ogul[84], Y. Onel, F. Ozok[85], A. Penzo, C. Snyder, E. Tiras, J. Wetzel, K. Yi[86]

Johns Hopkins University, Baltimore, U.S.A.

O. Amram, B. Blumenfeld, L. Corcodilos, M. Eminizer, A.V. Gritsan, S. Kyriacou, P. Maksimovic, C. Mantilla, J. Roskes, M. Swartz, T.Á. Vámi

The University of Kansas, Lawrence, U.S.A.

C. Baldenegro Barrera, P. Baringer, A. Bean, A. Bylinkin, T. Isidori, S. Khalil, J. King, G. Krintiras, A. Kropivnitskaya, C. Lindsey, W. Mcbrayer, N. Minafra, M. Murray, C. Rogan, C. Royon, S. Sanders, E. Schmitz, J.D. Tapia Takaki, Q. Wang, J. Williams, G. Wilson

Kansas State University, Manhattan, U.S.A.

S. Duric, A. Ivanov, K. Kaadze, D. Kim, Y. Maravin, D.R. Mendis, T. Mitchell, A. Modak, A. Mohammadi

Lawrence Livermore National Laboratory, Livermore, U.S.A.

F. Rebassoo, D. Wright

University of Maryland, College Park, U.S.A.

E. Adams, A. Baden, O. Baron, A. Belloni, S.C. Eno, Y. Feng, N.J. Hadley, S. Jabeen, G.Y. Jeng, R.G. Kellogg, T. Koeth, A.C. Mignerey, S. Nabili, M. Seidel, A. Skuja, S.C. Tonwar, L. Wang, K. Wong

Massachusetts Institute of Technology, Cambridge, U.S.A.

D. Abercrombie, B. Allen, R. Bi, S. Brandt, W. Busza, I.A. Cali, Y. Chen, M. D'Alfonso, G. Gomez Ceballos, M. Goncharov, P. Harris, D. Hsu, M. Hu, M. Klute, D. Kovalskyi, J. Krupa, Y.-J. Lee, P.D. Luckey, B. Maier, A.C. Marini, C. Mcginn, C. Mironov, S. Narayanan, X. Niu, C. Paus, D. Rankin, C. Roland, G. Roland, Z. Shi, G.S.F. Stephans, K. Sumorok, K. Tatar, D. Velicanu, J. Wang, T.W. Wang, B. Wyslouch

JHEP08(2020)139

University of Minnesota, Minneapolis, U.S.A.

R.M. Chatterjee, A. Evans, S. Guts[†], P. Hansen, J. Hiltbrand, Sh. Jain, M. Krohn, Y. Kubota, Z. Lesko, J. Mans, M. Revering, R. Rusack, R. Saradhy, N. Schroeder, N. Strobbe, M.A. Wadud

University of Mississippi, Oxford, U.S.A.

J.G. Acosta, S. Oliveros

University of Nebraska-Lincoln, Lincoln, U.S.A.

K. Bloom, S. Chauhan, D.R. Claes, C. Fangmeier, L. Finco, F. Golf, J.R. González Fernández, I. Kravchenko, J.E. Siado, G.R. Snow[†], B. Stieger, W. Tabb

State University of New York at Buffalo, Buffalo, U.S.A.

G. Agarwal, C. Harrington, I. Iashvili, A. Kharchilava, C. McLean, D. Nguyen, A. Parker, J. Pekkanen, S. Rappoccio, B. Roozbahani

Northeastern University, Boston, U.S.A.

G. Alverson, E. Barberis, C. Freer, Y. Haddad, A. Hortiangtham, G. Madigan, B. Marzocchi, D.M. Morse, V. Nguyen, T. Orimoto, L. Skinnari, A. Tishelman-Charny, T. Wamorkar, B. Wang, A. Wisecarver, D. Wood

Northwestern University, Evanston, U.S.A.

S. Bhattacharya, J. Bueghly, Z. Chen, A. Gilbert, T. Gunter, K.A. Hahn, N. Odell, M.H. Schmitt, K. Sung, M. Velasco

University of Notre Dame, Notre Dame, U.S.A.

R. Bucci, N. Dev, R. Goldouzian, M. Hildreth, K. Hurtado Anampa, C. Jessop, D.J. Karmgard, K. Lannon, W. Li, N. Loukas, N. Marinelli, I. Mcalister, F. Meng, K. Mohrman, Y. Musienko[42], R. Ruchti, P. Siddireddy, S. Taroni, M. Wayne, A. Wightman, M. Wolf, L. Zygala

The Ohio State University, Columbus, U.S.A.

J. Alimena, B. Bylsma, B. Cardwell, L.S. Durkin, B. Francis, C. Hill, W. Ji, A. Lefeld, B.L. Winer, B.R. Yates

Princeton University, Princeton, U.S.A.

G. Dezoort, P. Elmer, N. Haubrich, S. Higginbotham, A. Kalogeropoulos, G. Kopp, S. Kwan, D. Lange, M.T. Lucchini, J. Luo, D. Marlow, K. Mei, I. Ojalvo, J. Olsen, C. Palmer, P. Piroué, D. Stickland, C. Tully

University of Puerto Rico, Mayaguez, U.S.A.

S. Malik, S. Norberg

Purdue University, West Lafayette, U.S.A.

V.E. Barnes, R. Chawla, S. Das, L. Gutay, M. Jones, A.W. Jung, B. Mahakud, G. Negro, N. Neumeister, C.C. Peng, S. Piperov, H. Qiu, J.F. Schulte, N. Trevisani, F. Wang, R. Xiao, W. Xie

JHEP08(2020)139

Purdue University Northwest, Hammond, U.S.A.
T. Cheng, J. Dolen, N. Parashar

Rice University, Houston, U.S.A.
A. Baty, S. Dildick, K.M. Ecklund, S. Freed, F.J.M. Geurts, M. Kilpatrick, A. Kumar, W. Li, B.P. Padley, R. Redjimi, J. Roberts†, J. Rorie, W. Shi, A.G. Stahl Leiton, Z. Tu, A. Zhang

University of Rochester, Rochester, U.S.A.
A. Bodek, P. de Barbaro, R. Demina, J.L. Dulemba, C. Fallon, T. Ferbel, M. Galanti, A. Garcia-Bellido, O. Hindrichs, A. Khukhunaishvili, E. Ranken, R. Taus

Rutgers, The State University of New Jersey, Piscataway, U.S.A.
B. Chiarito, J.P. Chou, A. Gandrakota, Y. Gershtein, E. Halkiadakis, A. Hart, M. Heindl, E. Hughes, S. Kaplan, O. Karacheban[21], I. Laflotte, A. Lath, R. Montalvo, K. Nash, M. Osherson, S. Salur, S. Schnetzer, S. Somalwar, R. Stone, S.A. Thayil, S. Thomas

University of Tennessee, Knoxville, U.S.A.
H. Acharya, A.G. Delannoy, S. Spanier

Texas A&M University, College Station, U.S.A.
O. Bouhali[87], M. Dalchenko, A. Delgado, R. Eusebi, J. Gilmore, T. Huang, T. Kamon[88], H. Kim, S. Luo, S. Malhotra, D. Marley, R. Mueller, D. Overton, L. Perniè, D. Rathjens, A. Safonov

Texas Tech University, Lubbock, U.S.A.
N. Akchurin, J. Damgov, V. Hegde, S. Kunori, K. Lamichhane, S.W. Lee, T. Mengke, S. Muthumuni, T. Peltola, S. Undleeb, I. Volobouev, Z. Wang, A. Whitbeck

Vanderbilt University, Nashville, U.S.A.
E. Appelt, S. Greene, A. Gurrola, R. Janjam, W. Johns, C. Maguire, A. Melo, H. Ni, K. Padeken, F. Romeo, P. Sheldon, S. Tuo, J. Velkovska, M. Verweij

University of Virginia, Charlottesville, U.S.A.
L. Ang, M.W. Arenton, B. Cox, G. Cummings, J. Hakala, R. Hirosky, M. Joyce, A. Ledovskoy, C. Neu, B. Tannenwald, Y. Wang, E. Wolfe, F. Xia

Wayne State University, Detroit, U.S.A.
P.E. Karchin, N. Poudyal, J. Sturdy, P. Thapa

University of Wisconsin — Madison, Madison, WI, U.S.A.
K. Black, T. Bose, J. Buchanan, C. Caillol, S. Dasu, I. De Bruyn, L. Dodd, C. Galloni, H. He, M. Herndon, A. Hervé, U. Hussain, A. Lanaro, A. Loeliger, R. Loveless, J. Madhusudanan Sreekala, A. Mallampalli, D. Pinna, T. Ruggles, A. Savin, V. Shang, V. Sharma, W.H. Smith, D. Teague, S. Trembath-reichert, W. Vetens

†: Deceased
1: Also at Vienna University of Technology, Vienna, Austria
2: Also at Department of Basic and Applied Sciences, Faculty of Engineering, Arab Academy for Science, Technology and Maritime Transport, Alexandria, Egypt

JHEP08(2020)139

3: Also at Université Libre de Bruxelles, Bruxelles, Belgium
4: Also at IRFU, CEA, Université Paris-Saclay, Gif-sur-Yvette, France
5: Also at Universidade Estadual de Campinas, Campinas, Brazil
6: Also at Federal University of Rio Grande do Sul, Porto Alegre, Brazil
7: Also at UFMS, Nova Andradina, Brazil
8: Also at Universidade Federal de Pelotas, Pelotas, Brazil
9: Also at University of Chinese Academy of Sciences, Beijing, China
10: Also at Institute for Theoretical and Experimental Physics named by A.I. Alikhanov of NRC 'Kurchatov Institute', Moscow, Russia
11: Also at Joint Institute for Nuclear Research, Dubna, Russia
12: Also at British University in Egypt, Cairo, Egypt
13: Now at Ain Shams University, Cairo, Egypt
14: Also at Purdue University, West Lafayette, U.S.A.
15: Also at Université de Haute Alsace, Mulhouse, France
16: Also at Erzincan Binali Yildirim University, Erzincan, Turkey
17: Also at CERN, European Organization for Nuclear Research, Geneva, Switzerland
18: Also at RWTH Aachen University, III. Physikalisches Institut A, Aachen, Germany
19: Also at University of Hamburg, Hamburg, Germany
20: Also at Isfahan University of Technology, Isfahan, Iran, Isfahan, Iran
21: Also at Brandenburg University of Technology, Cottbus, Germany
22: Also at Skobeltsyn Institute of Nuclear Physics, Lomonosov Moscow State University, Moscow, Russia
23: Also at Institute of Physics, University of Debrecen, Debrecen, Hungary, Debrecen, Hungary
24: Also at Physics Department, Faculty of Science, Assiut University, Assiut, Egypt
25: Also at Institute of Nuclear Research ATOMKI, Debrecen, Hungary
26: Also at MTA-ELTE Lendület CMS Particle and Nuclear Physics Group, Eötvös Loránd University, Budapest, Hungary, Budapest, Hungary
27: Also at IIT Bhubaneswar, Bhubaneswar, India, Bhubaneswar, India
28: Also at Institute of Physics, Bhubaneswar, India
29: Also at G.H.G. Khalsa College, Punjab, India
30: Also at Shoolini University, Solan, India
31: Also at University of Hyderabad, Hyderabad, India
32: Also at University of Visva-Bharati, Santiniketan, India
33: Also at Indian Institute of Technology (IIT), Mumbai, India
34: Also at Deutsches Elektronen-Synchrotron, Hamburg, Germany
35: Also at Department of Physics, University of Science and Technology of Mazandaran, Behshahr, Iran
36: Now at INFN Sezione di Bari[a], Università di Bari[b], Politecnico di Bari[c], Bari, Italy
37: Also at Italian National Agency for New Technologies, Energy and Sustainable Economic Development, Bologna, Italy
38: Also at Centro Siciliano di Fisica Nucleare e di Struttura Della Materia, Catania, Italy
39: Also at Riga Technical University, Riga, Latvia, Riga, Latvia
40: Also at Consejo Nacional de Ciencia y Tecnología, Mexico City, Mexico
41: Also at Warsaw University of Technology, Institute of Electronic Systems, Warsaw, Poland
42: Also at Institute for Nuclear Research, Moscow, Russia
43: Now at National Research Nuclear University 'Moscow Engineering Physics Institute' (MEPhI), Moscow, Russia
44: Also at Institute of Nuclear Physics of the Uzbekistan Academy of Sciences, Tashkent, Uzbekistan

JHEP08(2020)139

45: Also at St. Petersburg State Polytechnical University, St. Petersburg, Russia
46: Also at University of Florida, Gainesville, U.S.A.
47: Also at Imperial College, London, United Kingdom
48: Also at P.N. Lebedev Physical Institute, Moscow, Russia
49: Also at California Institute of Technology, Pasadena, U.S.A.
50: Also at Budker Institute of Nuclear Physics, Novosibirsk, Russia
51: Also at Faculty of Physics, University of Belgrade, Belgrade, Serbia
52: Also at Università degli Studi di Siena, Siena, Italy
53: Also at Trincomalee Campus, Eastern University, Sri Lanka, Nilaveli, Sri Lanka
54: Also at INFN Sezione di Pavia[a], Università di Pavia[b], Pavia, Italy, Pavia, Italy
55: Also at National and Kapodistrian University of Athens, Athens, Greece
56: Also at Universität Zürich, Zurich, Switzerland
57: Also at Stefan Meyer Institute for Subatomic Physics, Vienna, Austria, Vienna, Austria
58: Also at Laboratoire d'Annecy-le-Vieux de Physique des Particules, IN2P3-CNRS, Annecy-le-Vieux, France
59: Also at Şırnak University, Sirnak, Turkey
60: Also at Department of Physics, Tsinghua University, Beijing, China, Beijing, China
61: Also at Near East University, Research Center of Experimental Health Science, Nicosia, Turkey
62: Also at Beykent University, Istanbul, Turkey, Istanbul, Turkey
63: Also at Istanbul Aydin University, Application and Research Center for Advanced Studies (App. & Res. Cent. for Advanced Studies), Istanbul, Turkey
64: Also at Mersin University, Mersin, Turkey
65: Also at Piri Reis University, Istanbul, Turkey
66: Also at Adiyaman University, Adiyaman, Turkey
67: Also at Ozyegin University, Istanbul, Turkey
68: Also at Izmir Institute of Technology, Izmir, Turkey
69: Also at Necmettin Erbakan University, Konya, Turkey
70: Also at Bozok Universitetesi Rektörlügü, Yozgat, Turkey
71: Also at Marmara University, Istanbul, Turkey
72: Also at Milli Savunma University, Istanbul, Turkey
73: Also at Kafkas University, Kars, Turkey
74: Also at Istanbul Bilgi University, Istanbul, Turkey
75: Also at Hacettepe University, Ankara, Turkey
76: Also at Vrije Universiteit Brussel, Brussel, Belgium
77: Also at School of Physics and Astronomy, University of Southampton, Southampton, United Kingdom
78: Also at IPPP Durham University, Durham, United Kingdom
79: Also at Monash University, Faculty of Science, Clayton, Australia
80: Also at Bethel University, St. Paul, Minneapolis, U.S.A., St. Paul, U.S.A.
81: Also at Karamanoğlu Mehmetbey University, Karaman, Turkey
82: Also at Bingol University, Bingol, Turkey
83: Also at Georgian Technical University, Tbilisi, Georgia
84: Also at Sinop University, Sinop, Turkey
85: Also at Mimar Sinan University, Istanbul, Istanbul, Turkey
86: Also at Nanjing Normal University Department of Physics, Nanjing, China
87: Also at Texas A&M University at Qatar, Doha, Qatar
88: Also at Kyungpook National University, Daegu, Korea, Daegu, Korea

JHEP08(2020)139